

Colour in context. Pigments and other coloured residues from the Early-Middle Holocene site of Takarkori (SW Libya)

Savino di Lernia · Silvia Bruni · Irina Cislaghi · Mauro Cremaschi ·
Marina Gallinaro · Vittoria Gugliemi · Anna Maria Mercuri ·
Giansimone Poggi · Andrea Zerboni

Received: 2 October 2014 / Accepted: 7 January 2015 / Published online: 6 March 2015
© Springer-Verlag Berlin Heidelberg 2015

Abstract We present the multidisciplinary investigation of pigments and artefacts with traces of colour from the Early-Middle Holocene site of Takarkori, located in the Tadrart Acacus Mountains (central Sahara, SW Libya). Here, geological, archaeological, taphonomic and chemical studies (Raman, Fourier-transform infrared, X-ray powder diffraction, gas chromatography–mass spectrometry) are used to examine a vast range of artefacts (raw materials, grinding stones, painted items, as well as lithic, bone, wooden and ceramic tools) equally distributed from Late Acacus contexts related to hunter-gatherers (ca. 8900–7400 uncal years bp) to pastoral groups (ca. 7400–4500 uncal years bp). The exploited minerals

(goethite, hematite, kaolinite and jarosite, among others) are locally procured and processed using quartzarenite grinding stones of different shapes and sizes. Thermal treatment of the minerals is also suggested by X-ray powder diffraction (XRD) and Raman studies. Gas chromatography–mass spectrometry (GC-MS) analyses show the addition of a lipid binder to small lumps of pigments in order to obtain a sticky product. Their fatty acid distribution differs from the residues on grinding stones, pointing to a specific use of these lumps. The grinding stones have also been used to crush and pulverize the pigments and as base for colour preparation. A sample of colour from a fallen painted slab referable to late pastoral phases shows the

Electronic supplementary material The online version of this article (doi:10.1007/s12520-015-0229-4) contains supplementary material, which is available to authorized users.

S. di Lernia (✉)
Dipartimento di Scienze dell'Antichità, Sapienza Università di Roma,
Via dei Volsci 122, 00185 Rome, Italy
e-mail: savino.dilemia@uniroma1.it

S. di Lernia
School of Geography, Archaeology and Environmental Studies,
University of the Witwatersrand, Private Bag 3, Johannesburg 2050,
South Africa

S. Bruni · I. Cislaghi · V. Gugliemi
Dipartimento di Chimica, Università degli Studi di Milano, via C.
Golgi 19, 20133 Milan, Italy

S. Bruni
e-mail: silvia.bruni@unimi.it

M. Cremaschi · A. Zerboni
Dipartimento di Scienze della Terra 'Ardito Desio', Università degli
Studi di Milano, via L. Mangiagalli 34, 20133 Milan, Italy

M. Cremaschi
e-mail: mauro.cremaschi@unimi.it

A. Zerboni
e-mail: andrea.zerboni@unimi.it

M. Gallinaro · G. Poggi
The Archaeological Mission in the Sahara, Sapienza Università di
Roma, Rome, Italy

M. Gallinaro
Dipartimento di Storia, Scienze dell'Uomo e della Formazione,
Università di Sassari, Sassari, Italy
e-mail: marina.gallinaro@uniss.it

A. M. Mercuri
Laboratorio di Palinologia e Paleobotanica, Dipartimento di Scienze
della Vita, Università di Modena e Reggio Emilia, Viale Caduti in
Guerra, 127, 41121 Modena, Italy
e-mail: annamaria.mercuri@unimore.it

presence of a binder, chemically identified as casein. Taken together, the evidence collected at Takarkori conveys to suggest an articulated *chaîne opératoire*, not only directed towards the preparation of pigments for the parietal rock art but also to other non-utilitarian functions, such as body care and ornamentation and decoration of artefacts.

Keywords Holocene · Sahara · Pigments · Foragers · Herders · Chemical analyses

Introduction

Despite the long tradition of study, we still have a limited knowledge of Saharan rock art. Unveiled to the western world in the nineteenth century (Barth 1857–1858), the study of paintings and engravings attracted since then generations of scholars, mostly focussing on the analysis of art styles and their chronological position (e.g. Mori 1965; Le Quellec 1998; Muzzolini 2001). More recently, many research programs embarked on a paradigm change, with increasing attempts to reinsert the Saharan artworks in their wider archaeological context, reconnecting the rock art evidence to the landscape where they are inscribed (e.g. di Lernia and Gallinaro 2010; Guagnin 2012; Gallinaro 2013; Kuper 2013).

In this paper, we have collected the evidence for artefacts with traces of coloured residues from the Early-Middle Holocene site of Takarkori (Tadrart Acacus Mountains, SW Libya), in an attempt to investigate their nature and potential relations with rock art through a multidisciplinary approach.

The effort to reconstruct the *chaîne opératoire* of the colour-making process and use is based on spatial and stratigraphic analysis of the assemblage, supported by radiocarbon chronology and cultural association, together with chemical analysis of the residues.

Despite the lack of direct evidence of artworks on the shelter walls, which are strongly affected by wind erosion, Takarkori indeed is a fortunate context. Differently from other Saharan sites, this context offers the opportunity to observe a long archaeological sequence, which encompasses the transition from Late Acacus foragers (ca. 8900–7400 uncal bp, ca. 8300–6100 BCE) to Pastoral herders (Early, Middle, and Late: ca. 7400–4500 uncal bp, ca. 6400–3000 BCE). Furthermore, the size of the excavation allowed the discovery of a large and diversified assemblage of artefacts with coloured residues (raw materials, grinding equipment, stone, bone, ceramic and wooden tools, and painted items), unparalleled in other Saharan contexts. Our research revealed that ochre and other minerals were intensively processed and used, not only to produce the pigments

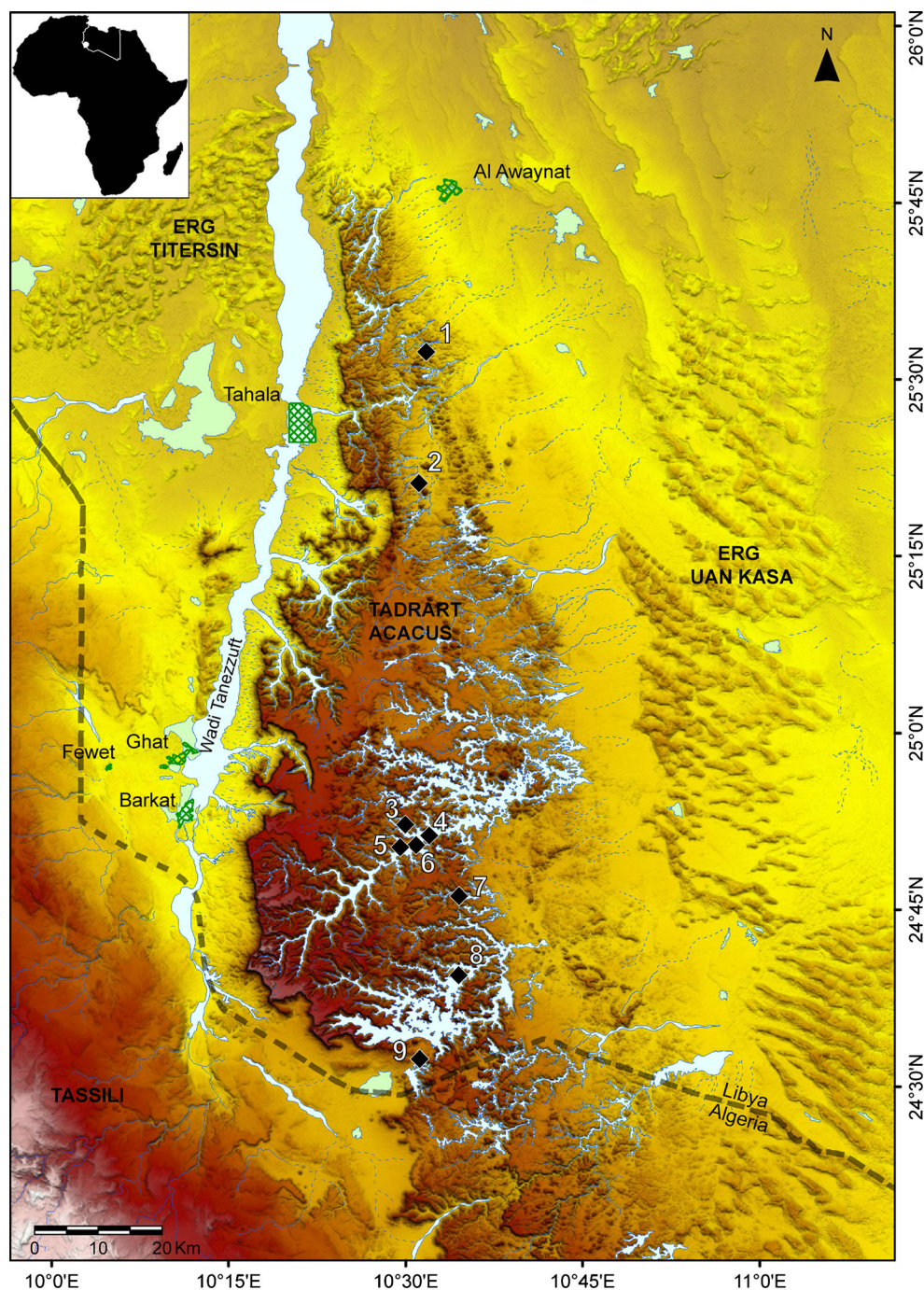
for the parietal rock art but also to be used for various non-utilitarian functions such as body care and ornamentation, decoration of stones, bone, ceramic artefacts and wooden sticks.

Pigments, colour and rock art in the Tadrart Acacus

The Tadrart Acacus massif is one of the main centres of rock art in the Sahara, known since the 1950s thanks to Fabrizio Mori (1965), and included in the UNESCO World Heritage list in 1985 (Fig. 1). The chronological and stylistic attribution of this artistic production is still debated. All authors agree on a Holocene age but diverge on the chronology of the earliest evidence and on stylistic definitions (e.g. di Lernia and Gallinaro 2011; Le Quellec 2013). The cavities punctuating the wadi banks host a rich corpus of paintings and engravings, analysed in the past by means of multidisciplinary perspectives (e.g. di Lernia and Zampetti 2008; Gallinaro 2013), with a particular emphasis on its preservation (di Lernia 2005; di Lernia and Gallinaro 2011). The state of preservation (poor/good) and the potential degree of contamination are elements of the utmost importance. These directly affect the quality of the pigments and the possibility to investigate the presence of organic binders, which are potentially suitable for radiocarbon dating (e.g. Mori et al. 2006; di Lernia 2012; Zerboni 2012). Previous chemical analyses carried out on the Acacus paintings highlighted the presence of organic (mostly proteic) matter, tentatively identified as milk casein (Mori 1965) and, more recently and on different samples, as similar to egg or serum albumin (Mori et al. 2006). As for the pigments, studies carried out in the past identified the presence of ochre (Mori 1965). X-ray fluorescence (XRF) analyses carried out on samples of pigments (red, yellow and white) manually scratched from the painted walls revealed the presence of a higher concentration of iron in the red sample and low calcium and high barium in the white sample, suggesting that the pigment did not have a carbonatic origin; the use of diatomaceous sediment or quartz was instead suggested (Moioli and Seccaroni 1992). However, these studies were not fully published, and the approach was not supported by a broader consideration of the regional context.

The use of pigments in the Acacus region is not only related to parietal rock art, but more rarely to portable artefacts, such as the painted pebble from Uan Amil (Ponti 1995). Grinding stones are the most common artefacts with traces of pigments. Several sites of Late Acacus and Pastoral age in the region yielded grinders with reddish and yellowish pigments, together with a few items on wood and bones. Lumps of red and yellow pigments were also recorded (e.g. Mori 1965; Barich and Mori 1970; Barich 1987; Cremaschi and di Lernia 1998; Garcea and

Fig. 1 The Tadrart Acacus (SW Libya), with Takarkori and other sites discussed in the text: Wadi Athal (1), Ti-n-Torha (2), Uan Afuda (3), Uan Tabu (4), Uan Amil (5), Uan Muhuggiag (6), Uan Telocat (7), Fozziagiaren (8) and Takarkori (9)



Sebastiani 1998; di Lernia 1999; Garcea 2001; di Lernia et al. 2013). Taken together, the largest part of coloured items in the Acacus is made of artefacts “active” in pigment processing (crushers, grinders, spatulas, etc.). “Passive” items, i.e. artefacts decorated with colour, are very rare. It is likely for this reason that the equation “ochre = rock art” routinely drove all interpretations in the past.

Human occupation at Takarkori

Opening towards the west, the rock shelter is on a terrace about 100 m above the wadi floor (Fig. 2). It is located on the southern side of wadi Takarkori, which separates the Tadrart Acacus from the Algerian Tadrart. The present surrounding vegetation is limited to desert savannah with *Acacia* trees (Mercuri 2008).

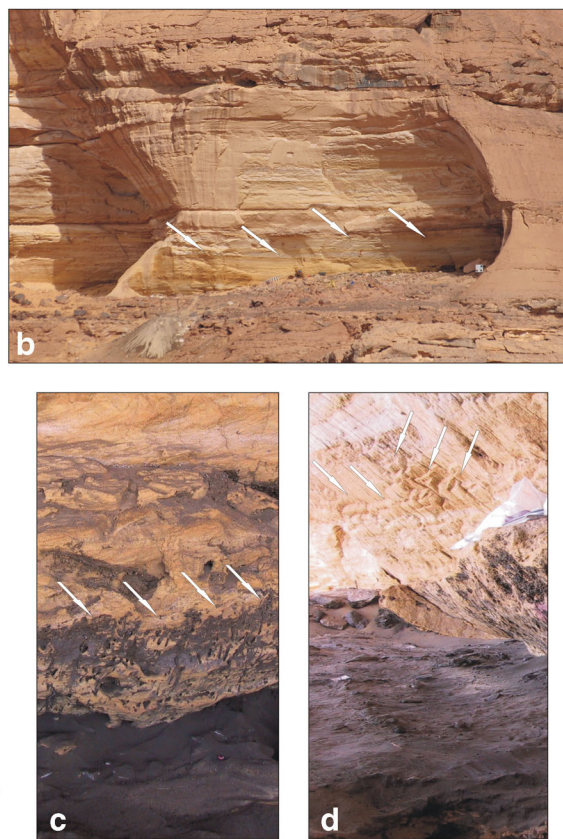
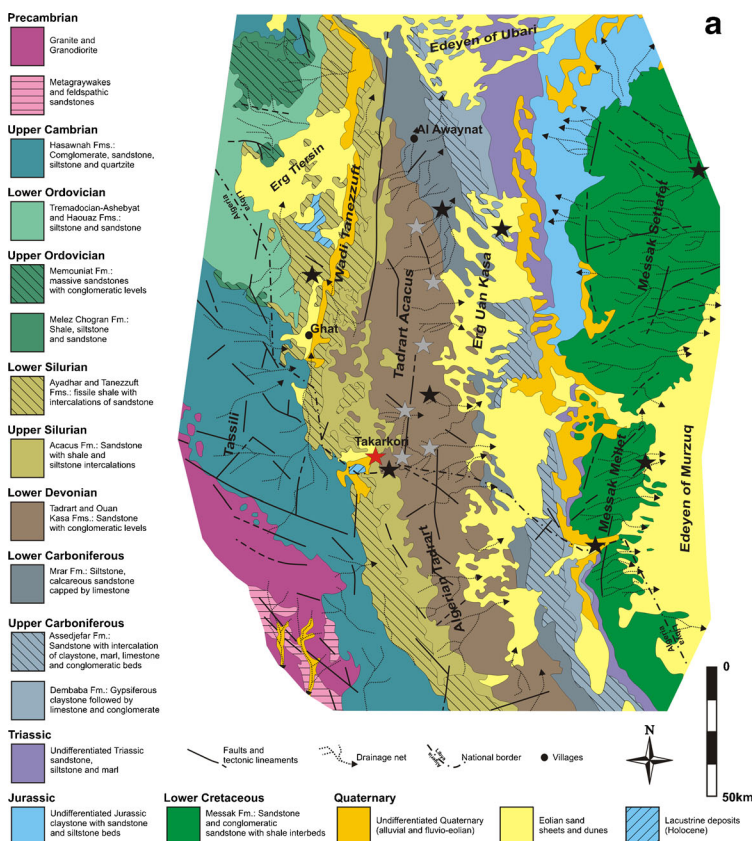


Fig. 2 **a** Geological map of the Tadrart Acacus region (modified from Galečić 1984; Jakovlječić 1984), with indication of the main rock formations (Fm.). The red star shows the position of Takarkori rock shelter. The black stars represent the main outcrops of rubified paleosols rich in Fe-bearing oxides, whereas the grey ones are the Fe-rich speleothems (see text for details). The Silurian shales of the Tanezzuft Fm. are the richest in iron oxides and hydroxides. **b** General view of

Takarkori rock shelter showing the general state of preservation of the vault; arrows show the brilliant yellow to whitish colour of the sandstone, which is typical of a freshly eroded rock surface. **c** A detail of the inner part of the rock shelter displaying strong erosion due to bioturbation (limits indicated by the arrows). **d** Evidence of thermal shattering on the vault (arrows)

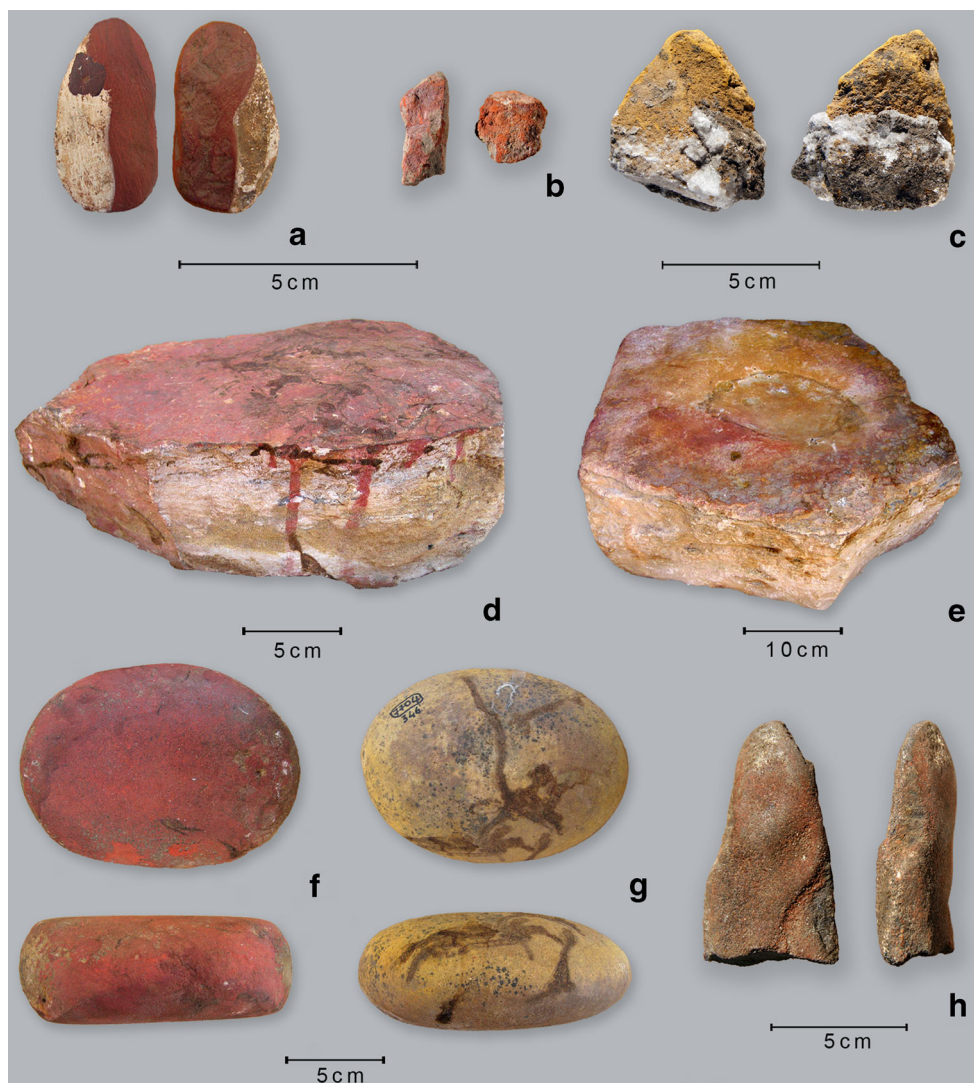
Table 1 Distribution of artefacts with colour residues, by cultural phase

Phase	Age ^a		Lumps/raw	Grinding equipment		Stones with coloured residues			Other items with coloured residues			Painted items			Total
	bp	BCE		LGS	UGS	Knapped stone	Stone	Smoothed stone	Bone	Wood	Ceramic	Rock wall fragment	Slab	Pebble	
LA1	8900–8500	8300–7500	1	5	0	0	0	0	0	0	0	0	0	0	6
LA2	8500–7900	7590–6650	3	26	8	4	1	0	0	0	1	0	0	43	
LA3	7900–7400	7000–6100	2	45	17	4	2	1	1	1	0	0	0	73	
EP1	7400–6900	6400–5700	7	25	17	2	3	0	4	0	0	0	1	58	
EP2	6900–6400	5890–5300	4	8	6	0	0	0	2	0	0	0	0	20	
MP1	6100–5500	5200–4250	2	4	3	0	1	0	0	0	0	0	0	10	
MP2	5500–5000	4450–3700	3	22	5	3	1	0	1	0	1	0	1	37	
LP1	5000–4000	3900–2350	0	4	1	1	0	0	0	0	0	1	1	8	
Total	–	–	22	139	57	14	8	1	8	1	1	2	1	2	256

LA Late Acacus, EP Early Pastoral, MP Middle Pastoral, LP Late Pastoral, LGS lower passive grinding stone, UGS upper active grinding stone

^aUncalibrated years bp (for the full set of C14 dates, see Cherkinsky and di Lernia 2013; Calibration has been done using OxCal Online v. 4.1 by Bronk Ramsey 2009 indicating the largest interval)

Fig. 3 Lumps and residues of colour on grinding equipment. Lumps: **a** L12 phase EP1, **b** L16 phase EP2 and **c** L11 phase EP1. Grinding equipment—LGS: **d** GE63 phase LA3 and **e** GE72 phase LA3, and UGS: **f** GE155 phase LA3, **g** GE170 phase EP1 and **h** GE181 phase EP1. Photo by S. Giovannetti



The site underwent extensive and stratigraphic excavations from 2003 to 2006 (Biagetti and di Lernia 2013; Cherkinsky and di Lernia 2013; Cremaschi et al. 2014). The terrace was first occupied by Late Acacus foragers from around 8900 to 7400 uncal bp (subdivided in three distinct units: LA1, 2, 3; see Table 1). Early Pastoral groups entered the site around 7400 uncal bp (EP1). Besides the use of the shelter as living area, there was a systematic use of the site as burial ground until the end of the EP2 phase, around 6400 uncal bp (Tafuri et al. 2006; di Lernia and Tafuri 2013). Middle Pastoral herders fully exploiting cattle resources are signalled in the site from around 6100 uncal bp (MP1) up to the mature phases (MP2). The last phases of occupation are marked by the presence of Late Pastoral groups, from around 5000 to 4500 uncal bp (LP1).

Unfortunately, the parietal art of this site, as in many rock shelters, is no longer preserved (but for the few items

collapsed from the vault). The vault is in fact characterized by an irregular and friable surface, the outcome of several millennia of weathering, also in relation to its opening to the west, which is strongly exposed to the dominant winds, rich in abrasive dust (Fig. 2).

Materials and methods

Methods of excavations, sampling and inventory

The excavation followed standard stratigraphic techniques, supported by the digital post processing, in a 3D environment, of archaeological contexts and materials (Biagetti and di Lernia 2013). All the materials showing traces of colour have been positioned through an electronic total station (ETS).

The sampling was planned on the basis of the following criteria: (i) colour range (using the Munsell® Soil Color Chart, see ESM 1), (ii) materials and blanks, and (iii) stratigraphic contexts and cultural phases. In order to minimize damage, the removal of coloured residues was carried out on grinding equipment and other stone materials only. Sampling was carried out in Libya by manual scratching with a metallic blade of an area of about 20×20 mm. The powder was immediately sealed in sterile vials, then transported in Italy, for which all the necessary permissions granted by the Libyan Department of Antiquities to Sapienza University of Rome had been obtained.

The inventory of pigment lumps and items with coloured residues is reported in ESM 1. Each item was labelled (ID) with its position (square), type of archaeological context (following Biagetti and di Lernia 2013) and cultural phase. Category and type of artefacts are detailed, together with raw material used, state of preservation and colour of the residues (using the Munsell© Soil Color Chart code). The state of preservation varies from 1 (fragments <25 % of the original size) to 4 (intact, or still >75 % of the original size). The area of coloured residues on the surface of the artefacts is expressed with values from 1 (<25 % of the surface) to 4 (>75 % of the surface).

Chemical analyses

Nineteen lumps of pigments and 49 coloured residues on artefacts were investigated by means of different analytical procedures, such as Fourier-transform infrared (FTIR) and Raman spectroscopies, X-ray powder diffraction (XRD) and visible–near-infrared (NIR) reflection spectroscopy. Scanning

electron microscopy–energy dispersive X-ray (SEM-EDX) analysis was used to identify the pigment on an avifauna bone. Gas chromatography–mass spectrometry (GC-MS) was employed to analyse the possible organic components of ten pigment lumps and of residues of colours on three different artefacts. Methodological aspects are detailed in ESM 2.

Results

The archaeological assemblage: contexts, taphonomy and features

Coloured items or traces of colour have been identified on several classes of materials throughout the archaeological sequence (Table 1): (i) raw materials, (ii) grinding equipment, (iii) stones with coloured residues, (iv) other items with coloured residues (bone, wood, pottery) and (v) painted items. The distinction between artefacts with coloured residues and painted items is quite labile, largely due to their state of preservation. Here, we followed a conservative approach, labelling as “painted” only those items with clear evidence of total coverage and/or depiction (e.g. horns and zoomorphic figures).

Raw material

Twenty-one lumps of coloured material have been brought to light (Fig. 3; ESM 1), mostly of reddish ($n=12$), and yellowish ($n=9$) colour. Usually of round shape, these crumbly and sticky lumps are small in size (up to 60 mm). They are present from the first occupation at Takarkori (absent in the Late Pastoral).

Table 2 Frequency of grinding equipment, including items with residues of colour, by cultural phase

	Lower grinding stones					Upper grinding stones				
	<i>n</i>	% ^a	Items with coloured residues			<i>n</i>	% ^a	Items with coloured residues		
			<i>n</i>	% ^b	% ^c on phase's assemblage			<i>n</i>	% ^b	% ^c on phase's assemblage
LA1	15	3.3	5	3.6	33.3	3	1.7	0	0	0.0
LA2	75	16.5	26	18.7	34.7	24	13.6	8	11.9	33.3
LA3	120	26.4	45	32.4	37.5	51	29.0	17	27.0	33.3
EP1	94	20.7	25	18.0	26.6	35	19.9	17	31.3	48.6
EP2	31	6.8	8	5.8	25.8	17	9.7	6	10.4	35.3
MP1	15	3.3	4	2.9	26.7	8	4.5	3	7.5	37.5
MP2	86	18.8	22	15.8	25.6	33	18.8	5	10.4	15.2
LP1	19	4.2	4	2.9	21.1	5	2.8	1	1.5	20.0
Total	455	100.0	139	30.5	–	176	100.0	57	32.4	–

^a The value shows the incidence of grinding tools within the cultural phase

^b The value shows the incidence of grinding tools with coloured residues within the cultural phase

^c The value indicates the ratio between grinding stones with coloured residues and the total of grinding tools of each cultural phase

Fig. 4 Spatial distribution of artefacts with coloured residues, by category and phase. **a** Late Acacus, **b** Early Pastoral, **c** Middle Pastoral and **d** Late Pastoral. Lumps of raw material: pigment (*solid asterisk*); bicolour nodule (*empty asterisk*). Grinding equipment, sized by state of preservation: LGS (*solid circle*), UGS (*empty circle*). Stones with colours: knapped stone (*solid triangle*) and stone (*empty triangle*); plaque on schist (*double triangle*). Other items with colour: bone (*solid square*), wood (*empty square*) and ceramic (*concentric square*). Painted items: rock wall fragment and slab (*solid diamond*), and painted pebble (*empty diamond*). GIS elaboration by M. Gallinaro

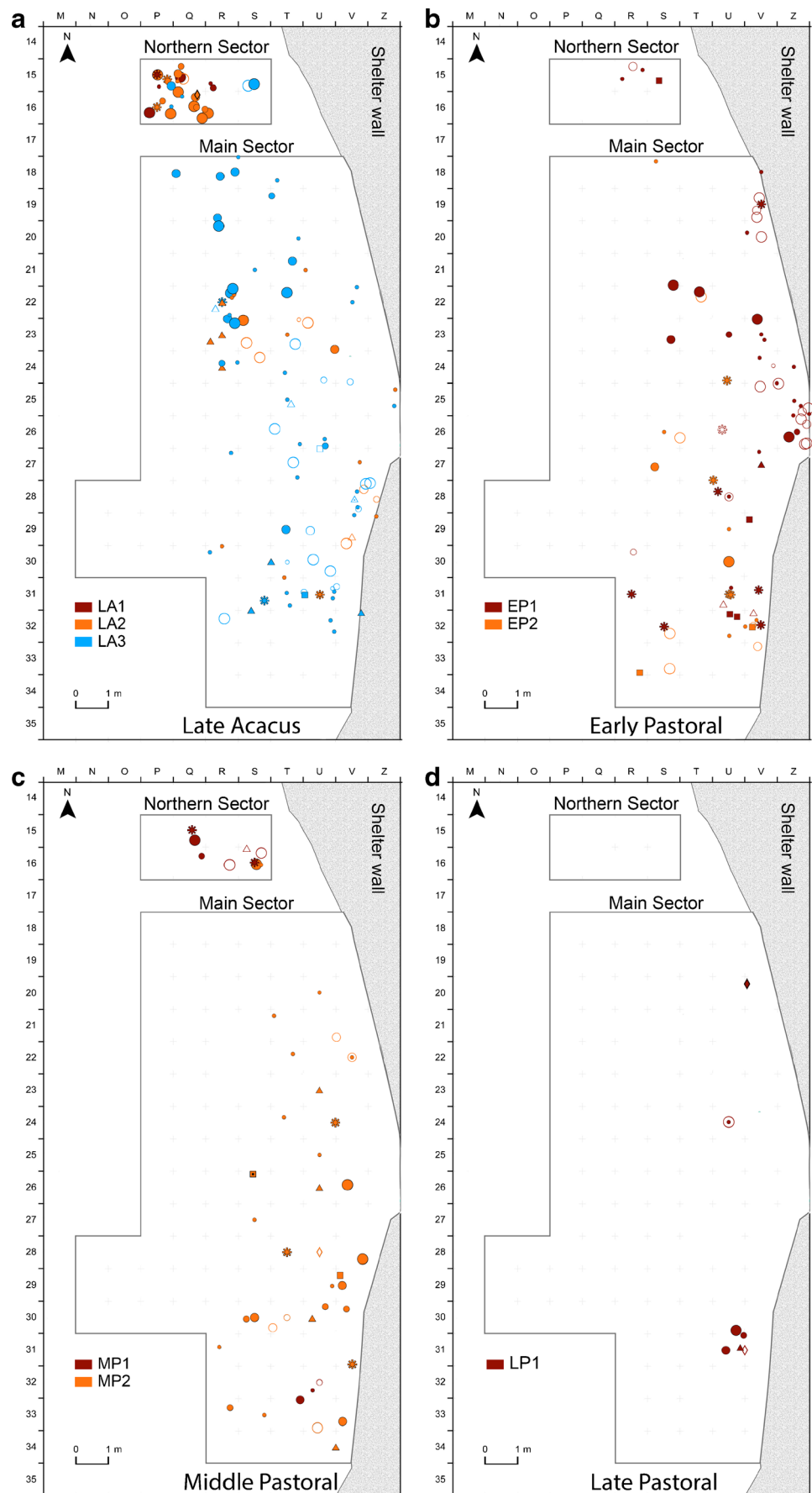


Table 3 Distribution of lower grinding stones with colour by archaeological contexts, phase and state of preservation

	Pit		Hearth ^a		Ash accumulation		Simple stone structure ^b		Complex stone structure ^c		Organic sand		Total	
	LGS	UGS	LGS	UGS	LGS	UGS	LGS	UGS	LGS	UGS	LGS	UGS	LGS	UGS
LA1							1		2		2		5	0
1 (<25 %)									1		1		2	
2 (25–50 %)									1				1	
3 (50–75 %)														
4 (75–100 %)							1				1		2	
LA2			2	2			3	3	13	1	8	2	26	8
1 (<25 %)			2	1			3		1		5		11	1
2 (25–50 %)								1	5				5	1
3 (50–75 %)								1	1		2		3	1
4 (75–100 %)				1				1	6	1	1	2	7	5
LA3			6	1	4	1	16	8	3		16	7	45	17
1 (<25 %)			4		3		8	1			13	1	28	2
2 (25–50 %)			1	1	1	1		1			1	2	3	5
3 (50–75 %)				1			3		3		1	1	8	1
4 (75–100 %)							5	6			1	3	6	9
EP1	1	1	1				11	8	3		9	8	25	17
1 (<25 %)	1						10	1			7	1	18	2
2 (25–50 %)		1	1				1						2	1
3 (50–75 %)								3	1			2	1	5
4 (75–100 %)								4	2		2	5	4	9
EP2			1								7	6	8	6
1 (<25 %)											6		6	0
2 (25–50 %)												1	1	1
3 (50–75 %)											1	1	1	1
4 (75–100 %)			1									4	1	4
MP1							1		2	1	1	2	4	3
1 (<25 %)									1				1	0
2 (25–50 %)										1	1		1	1
3 (50–75 %)									1				1	0
4 (75–100 %)							1					2	1	4
MP2	1		1					1	4		16	4	22	5
1 (<25 %)									1		11	1	12	0
2 (25–50 %)			1						2		1	2	4	1
3 (50–75 %)								1			3	1	3	3
4 (75–100 %)	1								1		1	1	3	1
LP1							2				2	1	4	1
1 (<25 %)											1		1	0
2 (25–50 %)							1						1	0
3 (50–75 %)							1						1	0
4 (75–100 %)											1	1	1	1
Total	2	1	11	3	4	1	34	20	27	2	61	30	139	57

^a Simple or structured^b Stone line, accumulation, arrangement^c Enclosure, platform, hut

Lumps are generally found in organic sands, more rarely from stone lines (EP1, $n=3$), floors (LA2, $n=1$) or ash accumulations (LA3, $n=1$). A naturally bi-coloured (white-red) nodule from EP1 layer shows traces of scraping (item L12). It is one of the pebbles found in the gravel bodies surrounding the Acacus massif and originating from the erosion of the shales belonging to the Tanezzuft Formation; the external white colour corresponds to a natural weathering rind. This item was likely used as raw material and therefore included here.

The grinding equipment

We unearthed more than 600 passive lower and active upper stones (Table 2; ESM 1). Their frequency is particularly high during LA3 and EP1, but recycling and reuse must be considered. Apart from the raw material used—always local quartzarenite with slightly different textures—shape, size and state of preservation greatly vary. However, intact (larger and heavier) lower stones appear to be more frequent in the Late Acacus levels (2 and 3), even if heavy (possibly reused) items are present also in EP2 and MP2 layers.

Coloured residues on the grinding equipment are common, nearly 1/3 of the assemblage: 139 passive lower stones (30.5 %) and 57 active upper stones (32.4 %) show traces of a vast range of red, yellow, orange, pink and white colours, plus a series of grading tones and sometimes a mix of different colours on the same artefact (Fig. 3; Table 2). We signal the fairly high incidence of upper grinding stones with traces of coloured residues in the EP1, where ca. 50 % of the artefacts show the presence of one or more colours. Such a high frequency of artefacts with coloured residues during the Early Pastoral reflects indeed a cultural aspect, given their wide-ranging distribution across the excavated area (Fig. 4). It could

also be related to the presence of burials, although the highly disturbed nature of the inhumation area prevented a secure association of some of these coloured items with a particular burial (di Lernia and Tafuri 2013).

From a taphonomic perspective (Table 3), grinding stones are either discarded (primary refuse) or de-functionalized and recycled in stone structures. In fact, most of the fragmented passive stones were found in organic sand ($n=61$; 43.9 %), followed by reuse of larger items in simple ($n=34$; 24.5 %) and complex stone structures ($n=27$; 19.4 %), including structured hearths ($n=11$; 7.9 %). The most intact, largest (>30 cm) and heaviest lower grinding stones, fully covered with colour, are present in all phases. Several of them were included as building elements (Fig. 4), such as the main structures of LA3 (squares T-Q/18-21) and LA2 phases (squares P-Q/15-16).

The upper grinding stones feature a different distribution by archaeological context. They are common in organic sand ($n=30$; 52.6 %), followed by their use within simple stone structures ($n=20$; 35.1 %), also including the stone accumulation approximately 1 m in depth next to the vault of the shelter, where many discarded objects are accumulated. In this case, understanding their spatial distribution is made difficult by the sin- and post-depositional disturbance processes, particularly several burials, which affected the area (di Lernia and Tafuri 2013).

Most of very fragmented grinding stones (value 1 < 25 %; see also ESM 1 for details of preservation values) are likely abandoned after breakage (the remains of colour normally do not cover the fracture), with a significant exception for the LA2 and LA3 phases, where some items (between 4.8 and 6 %) have been used for pigment preparation in a quite fragmented state (Table 4). A similar pattern can be envisaged for grinding stones with a preservation value of 2 (between 25 and 50 %) for the contexts dated to LA3 and EP1.

Table 4 Presence of colour over the fractures/edges of grinding stones, by phase and state of preservation

State of preservation	1 (<25 %)		2 (25–50 %)		3 (50–75 %)		4 (75–100 %)	
	No	Yes	No	Yes	No	Yes	No	Yes
LA1	2.4	0	3.7	0.0	0.0	0.0	1.8	1.8
LA2	9.5	4.8	22.2	0.0	10.3	3.4	19.3	1.8
LA3	29.8	6.0	22.2	7.4	27.6	3.4	26.3	0.0
EP1	22.6	1.2	3.7	7.4	6.9	13.8	22.8	1.8
EP2	6.0	1.2	0.0	3.7	6.9	0.0	8.8	0.0
MP1	1.2	0.0	7.4	0.0	0.0	3.4	5.3	0.0
MP2	7.1	7.1	14.8	3.7	10.3	10.3	7.0	0.0
LP1	1.2	0.0	3.7	0.0	3.4	0.0	1.8	1.8
Number of items	84		27		29		56	

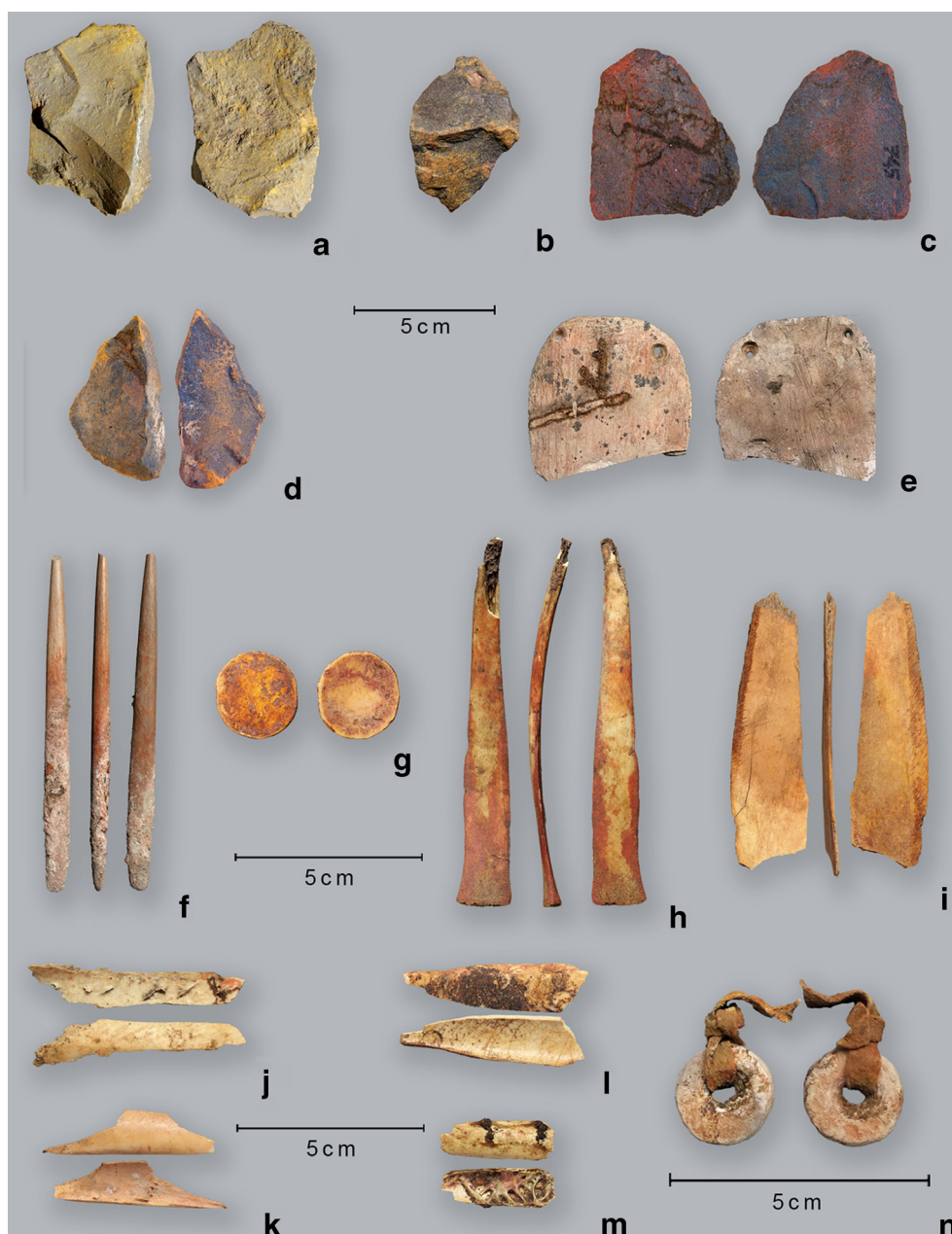
The disturbance processes due to the repeated use of the shelter and the opportunistic use of grindings tools, often reused and recycled, make difficult any spatial analysis. However, we can isolate at least four principal concentrations, which can be cautiously interpreted as remnants of processing areas. Two main concentrations can be envisaged during the LA3 phase (Fig. 4a). In the squares R-T/21-24 and S-U/29-32, we found clusters of grinding elements together with lumps of minerals and stone tools with coloured residues. An interesting distribution comes from the contexts dated to MP2 (squares S-V/28-30—Fig. 4c): fragments of lower and upper grinding stones, a lump of mineral, a stone scraper with red colour, a bird bone with drops of red colour and a broken red-

painted pebble. However, another significant distribution is evident in the Northern Sector, where since the earliest Late Acacus occupation phases (LA1 and LA2), lumps and lower grinding stones seem to be strictly associated. The widespread presence of grinding stones, during the EP1 (Fig. 4b), with a majority of active upper items, is also a noteworthy evidence of a functional use no more recognizable.

Other artefacts with coloured residues

Some traces of pigments were found on stone artefacts and other items such as bone, wooden and ceramic tools (Table 1; Fig. 5; ESM 1). The lithic tools are mainly

Fig. 5 Other artefacts with traces of colour. Lithics: **a** SC3 phase LA2, **b** SC4 phase LA2, **c** SC12 phase MP2, **d** SC13 phase MP2 and **e** SC23 phase LA3. Bones: **f** OIC1 phase LA3, **g** OIC2 phase EP1, **h** OIC6 phase EP2, **i** OIC7 phase EP2, **j** OIC3 phase EP1, **k** OIC4 phase EP1, **l** OIC5 phase EP1 and **m** OIC8 phase MP2. Ceramic: **n** OIC10 phase MP2. Photo by S. Giovannetti



flakes of silicified sandstone and show traces of red or yellow pigment, sometimes on both faces (ventral and dorsal), together with striations and use-wear traces visible at naked-eye, which suggest their use as scrapers. They are found in most cultural phases (but for LA1 and EP2) and in different stratigraphic contexts. A significant concentration is present in an accumulation of straw of the LA2 phase (ESM 1). No other spatial configuration is visible. One fragment of a stone ring made of shale (SC11), from an MP2 context, shows a few traces of red pigment on one surface, combined with striations and other use-wear traces, likely a residue from scraping. In a discard area of the LA3 phase, a fragmented thin plaque on shale (SC23: Fig. 5e) was found, showing traces of red colour. This artefact also features two holes, a series of notches on the edge and striations caused by scraping on both sides.

Eight bone artefacts of different phases (LA3 = n. 1, EP1 = n. 4, EP2 = n. 2, MP2 = n. 1), mostly found in organic sand, also bear traces of red colour. Two of them, a pointed projectile bone (OIC1: Fig. 5f) and a fragmented pointed item (OIC6: Fig. 5h), which were found discarded in ash accumulations, are extensively coloured in red. A circular flat bone disk ornament (OIC2: Fig. 5g) is coloured with red on both faces.

Interestingly, four of the bone artefacts exploited bird bones. These are light, sharp and pointed and show a few traces of pigment, either on the pointed tips or in the form of tiny drops on their surface (Fig. 5j-m).

A stick made of *Acacia* wood with remains of red pigment was found in a LA3 layer (Fig. 6; ESM 3). Unlike the spatula of *Calotropis* wood found at Uan Afuda (di Lernia 1999), which shows controlled burning and smoothing on the ends with thick traces of red

Fig. 6 **a** Tool made from *Acacia* wood with ochre. SEM photographs showing **b** the surface with ochre (much lighter) and **c** transverse section: diffuse-porous wood; vessels solitary and in radial rows of up to 4–5. **d** Vessel pits vary from oval to slit-like apertures. **e** A gum-like deposit is visible into the vessel

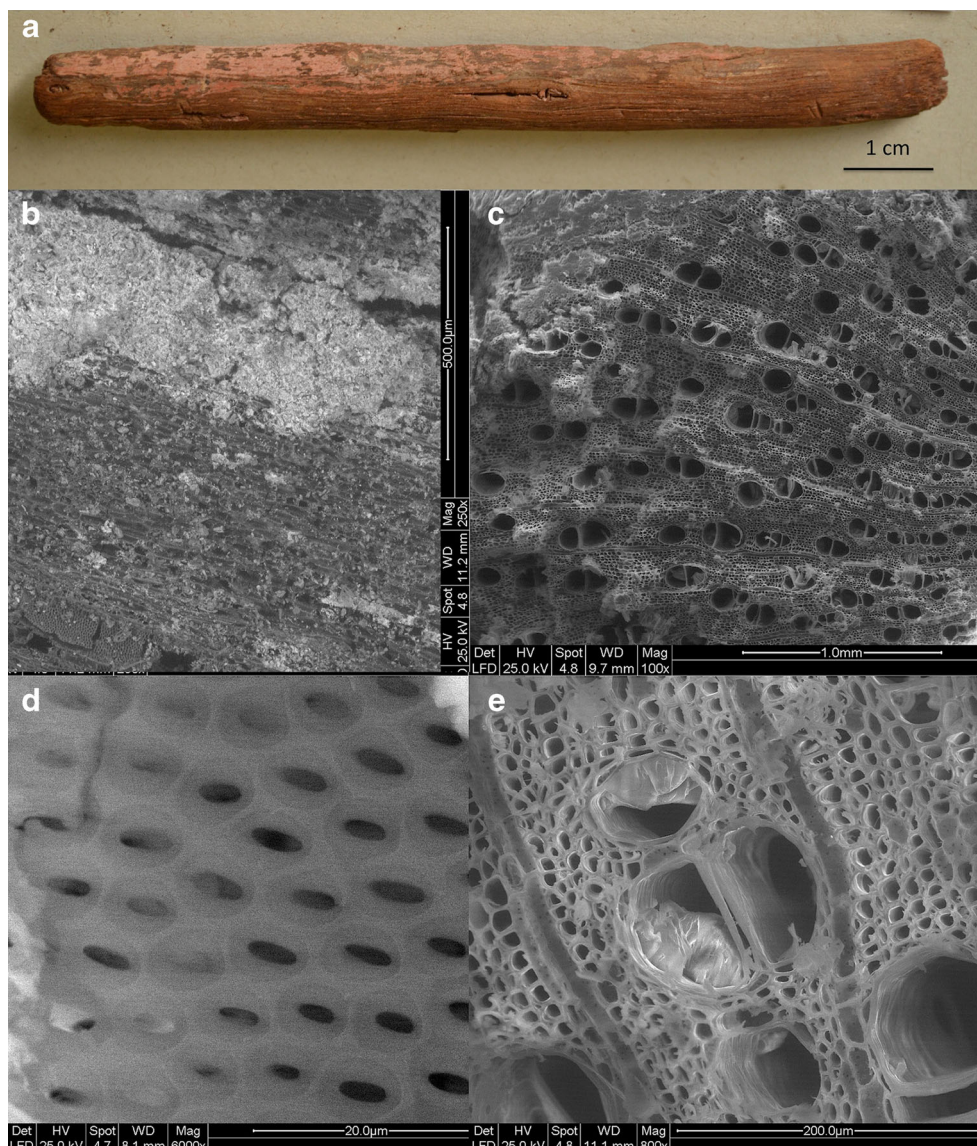
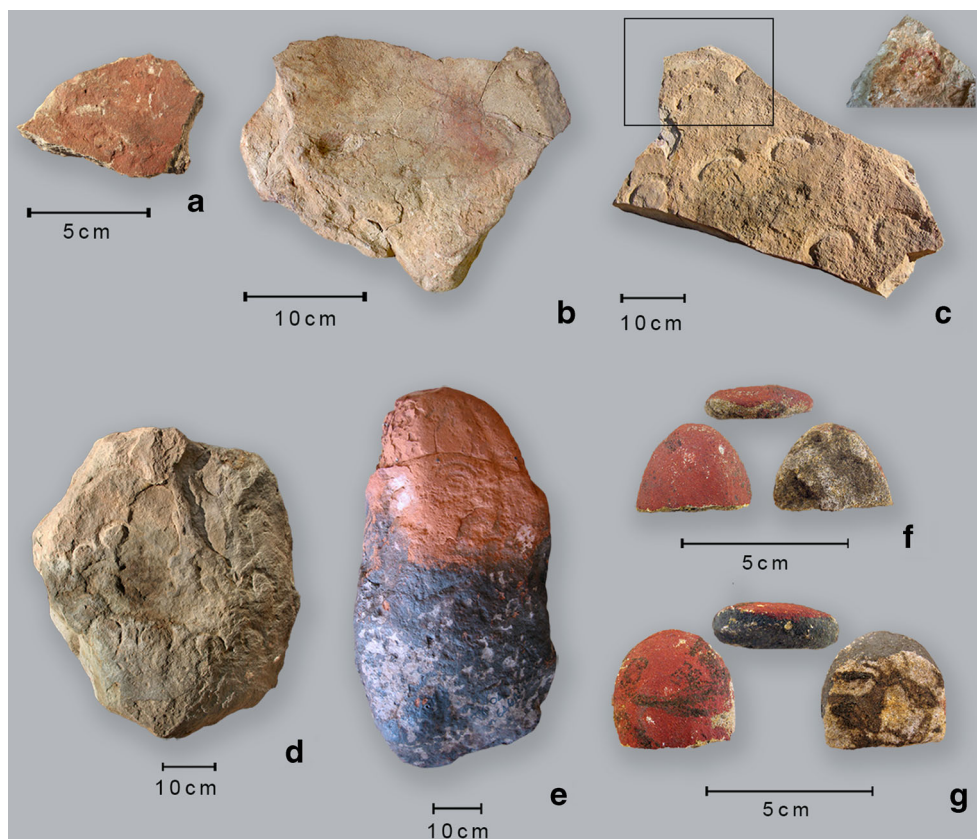


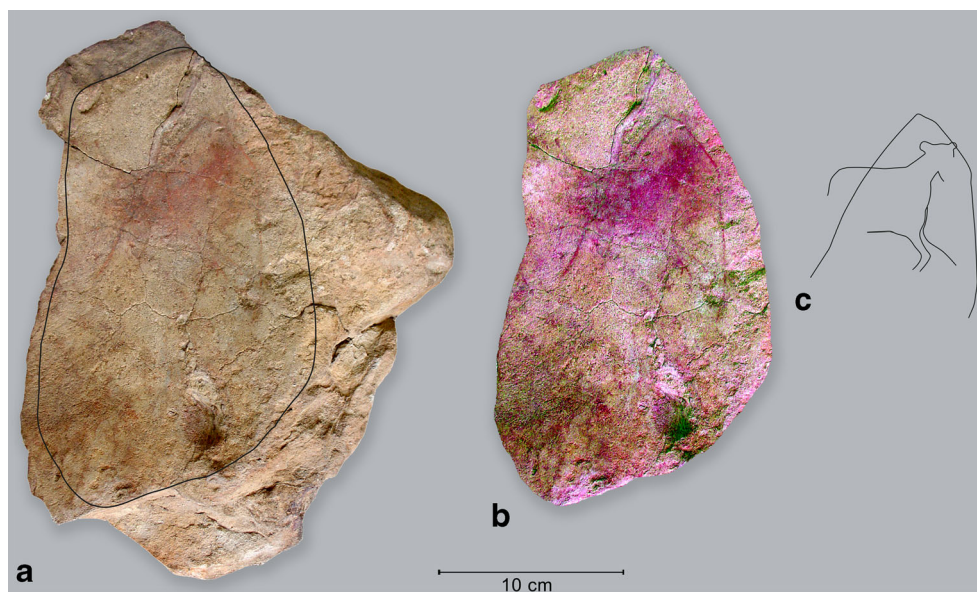
Fig. 7 Painted artefacts and other engraved stones. Rock wall fragments and engraved slab: **a** PI1 phase LA2, **b** PI2 phase LP1 and **c** PI3 phase EP1 (the rectangle indicates the position of the painted horn on the opposite side). Other engraved stones of EP1 phase (**d, e**). Painted pebbles: **f** PI4 phase MP2 and **g** PI5 phase LP1. Photo by S. Giovannetti



colour on one end and likely to have been used for painting, the stick from Takarkori seems to be a coloured item. As a matter of fact, even if poorly preserved, the remains of the red pigment are discontinuously present on all the external surface of the stick.

A pierced and smoothed small ceramic ring with a leather string still in its functional position was found in the organic sand of MP2 phase (OIC10: Fig. 5n). This personal ornament shows pale traces of bright brown colour on both sides.

Fig. 8 Digital enhancement of the painted rock wall fragment PI2: **a** original image, the *black contour line* shows the analysed area, **b** DStretch colour enhancement and **c** tracing of the highlighted paintings. Photo by S. Giovannetti; DStretch processing by M Gallinaro



Painted items

The retrieval in the archaeological deposits of slabs with traces of painting or engraving is not common. At Takarkori, the rock shelter wall is heavily eroded. Despite careful examination of all the stones, only two in fact show red coloured areas likely representing painted subjects, from LA2 and LP1 contexts (Fig. 7a and b: P11 and P12; Table 1; ESM 1). They both are fragments of the vault. The former is a tiny fragment (ca. $5 \times 7 \times 1.8$ cm) found scattered in the organic sand, showing unintelligible traces of red colour. The other element comes from a shallow pit close to the wall, consisting of a sub-triangular-shaped slab ($30.5 \times 35 \times 8$ cm). The most abundant trace of red colour extends from one end to the middle of the slab. The painting is barely visible, but the DStretch digital enhancement of faded colours (Harmann 2005–2013) was helpful (Fig. 8). Two superimposed subjects can be tentatively identified. The first is in plain red and appears to be a zoomorphic figure (ovicaprid?); the other is a linear trait, in pale red,

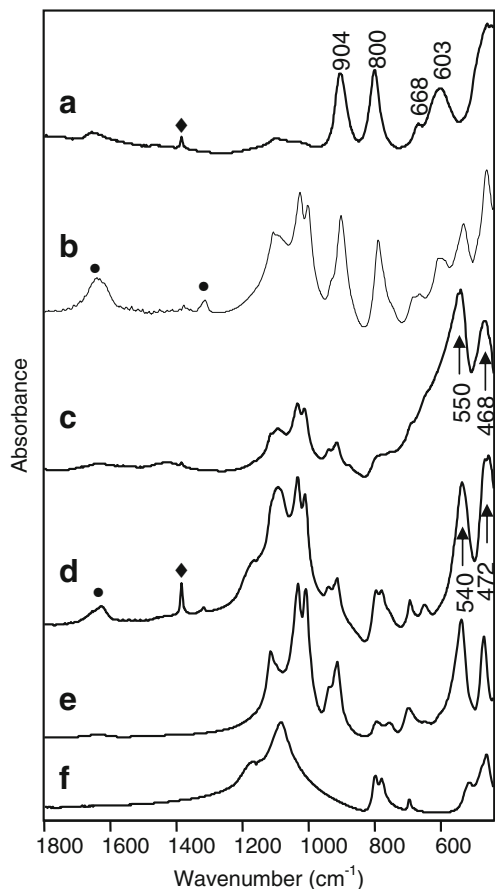


Fig. 9 FTIR spectra of yellow lump L9 (a), yellow pigment on grinding equipment GE27 (b), red lump L14 (c) and red pigment on stone SC16 (d). Wavenumbers are reported for bands characteristic of goethite and hematite. Spectra are also reported for kaolinite (e) and quartz (f), to be compared with those of the pigments (b–d), where bands due to the two minerals are well evident. (circle) Calcium oxalate hydrate and (diamond) potassium nitrate (see text)

possibly a semi-ovaloid line, and is superimposed on the animal. Even if the subjects are scarcely recognizable, the style of the zoomorphic figures and the uncertain contour line seem to suggest a chronological attribution to later pastoral phases.

One slab with a series of engraved horns also features a painted horn on the opposite face (Fig. 7c: P13). It was located out of the main excavation area sticking out of the Early Pastoral age (EP1) deposit. Other two stones with engraved horns were brought to light during the excavation, both of Early Pastoral age, supporting the chronological attribution of the engraved/painted one (Fig. 7d, e). Two pebbles fully covered with red colour come from MP2 and LP1 contexts (Fig. 7f, g).

Chemical analyses

Pigments

Lumps of raw material Yellow lumps proved to be composed of goethite α -FeO(OH), as an almost pure constituent or in mixture with kaolinite and quartz: Figs. 9 and 10 show respectively the characteristic FTIR and Raman bands of goethite (Gadsden 1975; van der Marel and Beutelspacher 1976; de

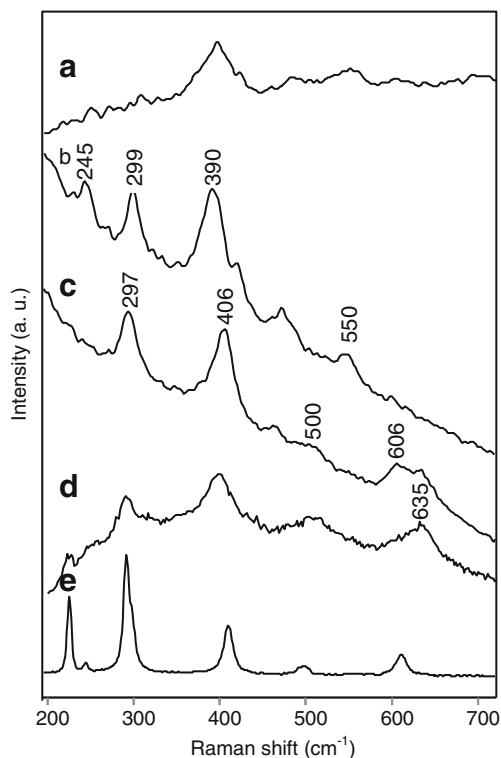


Fig. 10 Raman spectra of yellow lump L22 (a), yellow pigment on grinding equipment GE135 (b), red lump L3 (c) and red pigment on wooden stick OIC9 (d). Wavenumbers are reported for band characteristic of goethite and hematite. In order to compare the relative band intensities and bandwidths observed for the red pigments, the spectrum of α -Fe₂O₃ (e) is also shown. For a, $\lambda_{\text{exc}}=676$ nm; for b–e, $\lambda_{\text{exc}}=785$ nm

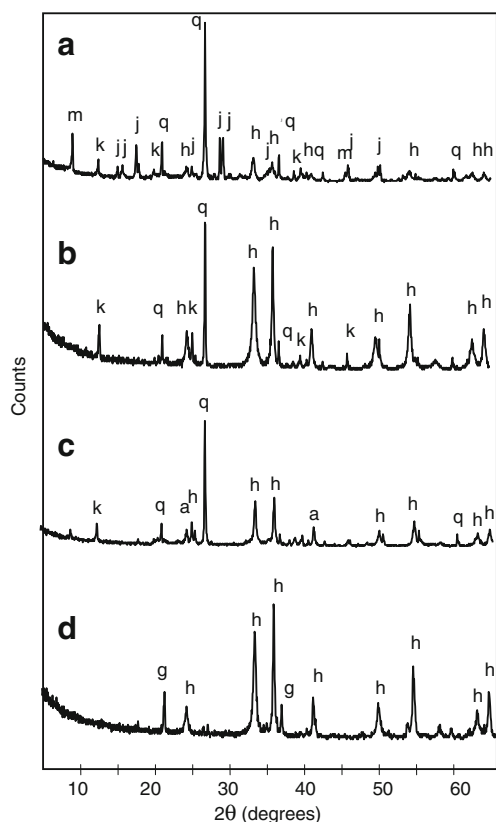


Fig. 11 Powder X-ray diffractograms of reddish-orange lump L20 (a), red lump L21 (b), red pigment on grinding equipment GE131 (c) and red outer layer of red-yellow lump L8 (d). *h* hematite, *g* goethite, *j* jarosite, *k* kaolinite, *q* quartz, *a* anatase, *m* mica

Faria et al. 1997; Bikiaris et al. 1999; Mortimore et al. 2004), observed in the spectra.

Due to the superposition of FTIR bands typical of hematite, at 570–550 and 468 cm^{-1} , with those due to kaolinite at 540 and 472 cm^{-1} (Gadsden 1975; van der Marel and Beutelspacher 1976), the presence of hematite in the red-coloured lumps can be inferred from FTIR spectra only by a greater intensity ratio between spectral components around 500 cm^{-1} and those around 1000 cm^{-1} in comparison with what was observed for kaolinite and quartz (Fig. 9), invariably detected in such lumps. For some of them, Raman spectra could be acquired (Fig. 10) and showed bands characteristic of hematite (de Faria et al. 1997; Bikiaris et al. 1999; Mortimore et al. 2004); otherwise, positive identification of the pigment was provided by XRD analysis (Fig. 11) and visible-NIR reflection spectra, exhibiting an edge at about 550 nm, a shoulder around 640 nm and a minimum at ca. 860 nm (Morris et al. 1985).

For the analysis of red lumps, it is worth noticing that for most samples, the XRD pattern shows an inversion between the intensities of (104) and (110) peaks, located respectively at 33.26° and 35.74°, in comparison with natural hematite (Fig. 11). At the same time, in the corresponding Raman

spectra, the 406- cm^{-1} band results to be stronger than the 297- cm^{-1} one, again in opposition to the spectral pattern of the natural pigment. These experimental data can be associated with a possible heating of goethite to obtain the red pigment at a temperature not higher than 400 °C, as reported in the literature both for Raman spectra (Kustova et al. 1992; de Faria and Lopes 2007) and X-ray diffractograms (Pomiès et al. 1998; Udda et al. 2000). In the case of Raman spectra, other authors (Gialanella et al. 2011) did not observe a variation in the relative intensity of the strongest bands of hematite when it was obtained from the heating of goethite, but just a broadening of the peaks, as well observed however in the spectra here reported for the red lumps. In any case, it was pointed out that the observed spectral features most properly indicate disordered hematite, which can also be associated with natural ores (Onoratini and Perinet 1985; Pomiès et al. 1998) or arise from other causes such as biodegradation and weathering (de Faria and Lopes 2007).

Among lumps of pigmented materials, two exceptions are represented by samples L20 and L8. The first one, of dark-reddish brown colour (Munsell® colour 2.5YR 3/4), is composed of jarosite $\text{KFe}_3(\text{OH})_6(\text{SO}_4)_2$ and hematite, as evidenced by the FTIR spectrum, where bands characteristic of jarosite were observed (ESM 4), and by XRD analysis, showing also peaks due to hematite (Fig. 11). The second sample had instead a yellow core surrounded by a red shell, and the core was found to be pure goethite from FTIR and Raman spectra, while the external layer contained both disordered hematite and goethite as shown by FTIR and XRD analyses (Fig. 11). Even if biodegradation or weathering cannot be ruled out, this particular sample could indeed represent a product of intentional but incomplete heating of a goethite lump, likely to transform the ochre from yellow into red.

Grinding equipment and stones with coloured residues For pigment residues sampled from grinding stones, FTIR spectra showed bands due to kaolinite, quartz and frequently calcium oxalates and/or nitrates (Fig. 9). In the case of yellow pigments, goethite was invariably identified through FTIR spectroscopy and, when not hindered by fluorescence, also on the basis of the Raman spectrum (Fig. 10). In red pigments, hematite could be easily recognized only when sufficient quantities of sample were available and then only by means of XRD for the reasons mentioned above (Figs. 9 and 11).

Other items with coloured residues The presence of hematite was finally confirmed also on two particular objects showing traces of red colour, namely the *Acacia* stick (sample OIC9) and an avifauna bone (sample OIC3).

The identification on the wooden stick was possible on the basis of the Raman signals (Fig. 10), again with an intensity inversion between the two bands located at lower

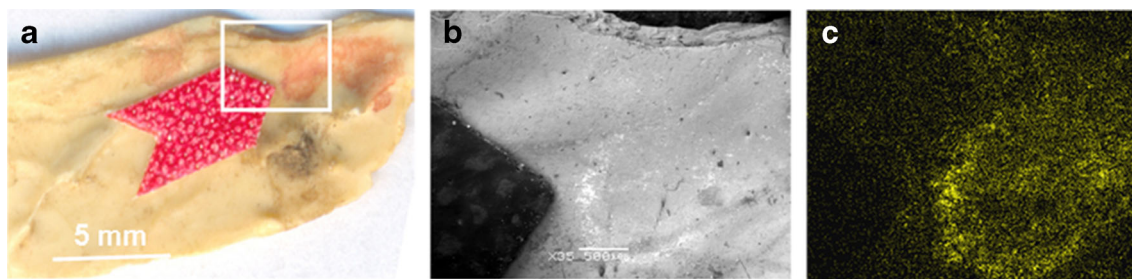


Fig. 12 **a** Avifauna bone OIC3 with red pigmented area (shown by the arrow). **b** SEM image (backscattered electrons) of the area in the square inset. **c** X-ray map of Fe in the same area. An evident correspondence is

observed among the red pigmented area on the object, the bright area in the SEM image and the region with higher Fe content in the X-ray map

wavenumbers. Moreover, a broad signal around 635 cm^{-1} is observed in the spectrum, which is similar to the overall pattern reported in the literature for goethite heated at temperatures ranging from 250 to 350 °C (de Faria and Lopes 2007), even if in this case, the above-cited band appears at the higher wavenumber of 657 cm^{-1} . A band around 635 cm^{-1} also appears, even if at weaker intensity, in the Raman spectra that could be obtained for some red lumps.

With regard to the red-stained avifauna bone, a Raman spectrum of the pigment could not be obtained, but the coincidence between the coloured area and the distribution of iron on the bone surface was demonstrated on the basis of X-ray maps obtained by SEM-EDX analysis (Fig. 12).

Organic components The sticky consistence of some of the pigment lumps prompted us to investigate the presence of organic components in ten samples (ESM 2). The GC-MS analysis of the extracts yielded a total weight fraction of fatty acids in the examined lumps from 100 to $200\text{ }\mu\text{g g}^{-1}$ (Table 5). A comparable content of lipids was determined in archaeological ochre pastes from Patagonia, dating to about 2000 years BP (Maier et al. 2007).

Moreover, the distribution of free fatty acids in our samples, also obtained from GC-MS analysis, showed two different patterns (Table 5 and Fig. 13), both different from that found for soil samples from the excavation site (usually largely dominated by palmitic acid $\text{C}_{16:0}$ and stearic acid $\text{C}_{18:0}$ in comparable amounts).

For six samples (L2, L3, L6, L7, L10 and L20), palmitic acid is predominant, while stearic acid is contained in a 1:2 ratio with respect to palmitic acid; tetradecanoic acid $\text{C}_{14:0}$ or dodecanoic acid $\text{C}_{12:0}$ follow in order of abundance. The lipid extracts of all these samples also contain appreciable amounts of oleic acid $\text{C}_{18:1}$. We encountered this distribution also for organic residues absorbed in potsherds from Takarkori and, together with the presence of a homologous series of *n*-alkanes, from C_{16} to C_{33} (odd-over-even carbon number predominance), it was considered diagnostic of plant oils (Dunne et al. 2012). It should be remarked, however, that for the pigment lumps, very limited amounts of *n*-alkanes were detected, with a prevalence of even carbon number terms. Moreover, appreciable quantities of dicarboxylic acids were observed just for sample L20.

A completely different distribution of fatty acids was encountered for the lipid extracts of the remaining four samples (L14, L16, L19 and L21), characterized by a remarkably high

Table 5 Relative weight percentages of fatty acids and weight fraction of lipid extract as determined by GC-MS for ten pigment lumps

Samples	Fatty acid relative percentage											Lipid concentration ($\mu\text{g g}^{-1}$)
	$\text{C}_{9:0}$	$\text{C}_{10:0}$	$\text{C}_{11:0}$	$\text{C}_{12:0}$	$\text{C}_{14:0}$	$\text{C}_{15:0}$	$\text{C}_{16:0}$	$\text{C}_{17:0}$	$\text{C}_{18:2}$	$\text{C}_{18:1}$	$\text{C}_{18:0}$	
L2	2.0	3.6	2.9	7.0	11.1	11.5	33.9	6.5	0.0	5.3	16.0	137
L3	1.8	3.5	2.5	7.9	12.9	11.4	29.6	6.3	0.1	6.9	17.2	99.9
L6	7.0	6.1	6.7	12.5	10.2	6.9	33.4	4.7	0.0	2.2	10.3	134
L7	5.5	3.5	0.9	5.2	9.0	5.9	36.2	1.7	0.2	13.1	18.6	122
L10	3.1	3.3	2.0	7.5	9.7	5.6	28.9	1.9	0.8	16.2	21.0	209
L14	29.6	13.6	7.4	13.8	5.2	3.9	13.2	1.5	-	2.5	9.3	162
L16	12.6	10.6	5.4	10.0	10.8	7.8	17.4	2.6	0.3	11.8	10.7	81.0
L19	14.6	10.5	7.3	12.7	8.3	5.8	19.7	2.3	0.2	6.7	12.1	122
L20	4.2	5.3	6.0	16.1	12.7	8.1	25.9	3.2	-	2.9	15.6	206
L21	36.2	17.2	8.5	10.6	3.7	2.3	9.9	0.7	0.1	1.6	9.2	135

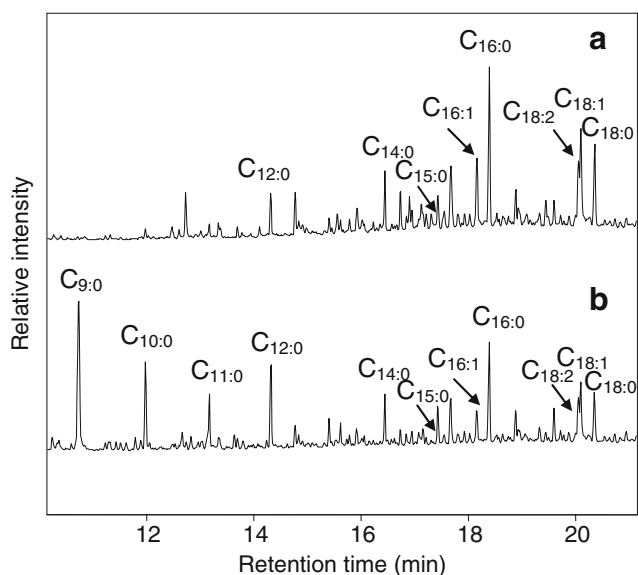


Fig. 13 Total ion current (TIC) chromatograms of the total lipid extract of sample L10 (a) and sample L14 (b). $C_{n,x}$ fatty acid with n carbon atoms and x double bond. Components are present as their TMS esters

relative percentage of nonanoic acid $C_{9:0}$, resulting in the prevailing component (or the second one in order of abundance). Moreover, especially for the two samples containing higher amounts of nonanoic acid, the ratio $C_{18:0}:C_{16:0}$ increases towards 1 and the amount of oleic acid $C_{18:1}$ decreases in comparison to the previously discussed group of lumps. The abundance of nonanoic acid is quite unusual for lipid residues in archaeological findings, but it has been reported for large pottery vessels dating to 900–720 BC, found in Syria and therefore in a similar arid environment (Shimoyama et al. 1995). It should be emphasized that, from a general point of view, the aridity of the context favours the preservation of shorter chain fatty acids (Regert et al. 1998; Copley et al. 2001, 2005). For those findings, it was suggested that nonanoic acid formed upon degradation of oleic acid, a process demonstrated to be favoured by the heating of oleic acid itself in the presence of clay minerals (Shimoyama et al. 1993). More generally, nonanoic acid was documented in the literature as oxidation product of oleic acid (Mittet 1980; Mills and White 1994).

The peculiar distribution of fatty acids reported for this second group of pigment lumps could therefore be attributed to a different or more degraded fat or oil, if compared to the first group. Recently, a catalytic effect of iron oxide on the degradation of vegetable and animal fats was indeed suggested (D'Elboux Bernardino et al. 2014). However, the hypothesis that those samples were subjected to heating, intentionally or accidentally, cannot be discarded. Quite interestingly, all the four lumps with a large content of nonanoic acid are red-pigmented, thus suggesting the possibility that lumps of yellow pigment, previously mixed with a fat or an oil, were subsequently heated to change their hue into red.

The fatty acid distribution was analysed qualitatively also for two other pigment samples, one from a grinding equipment and the other from a painted pebble (Table 6), resulting quite different from that of the lumps. Indeed, comparable amounts of palmitic and stearic acid, rather low quantities of medium-chain acids and similar amounts of dicarboxylic acids, were detected for these samples. The organic component of pigments from other grinding stones could not be investigated, due the low quantities of such samples.

The ten lumps examined for their lipid content were also analysed by GC-MS to check the presence of a proteinaceous component through their amino acid distribution. In all cases, a really low weight percentage of amino acids was detected, ranging from 0.005 to 0.04 % and therefore one to two order of magnitude lower than the amounts usually accepted in the literature as indicative of the presence of a proteinaceous binder (Rampazzi et al. 2002, 2007). Thus, the protein component of the examined samples seems to be practically negligible.

For comparison, one sample from a red area of the painted slab (sample PI2) was analysed for the possible presence of a proteinaceous organic binder. The protein content of the sample was 4 %, and the amino acid distribution indicated the use of a casein-based binder, most probably derived from milk, as evidenced by a comparison based on linear discriminant analysis

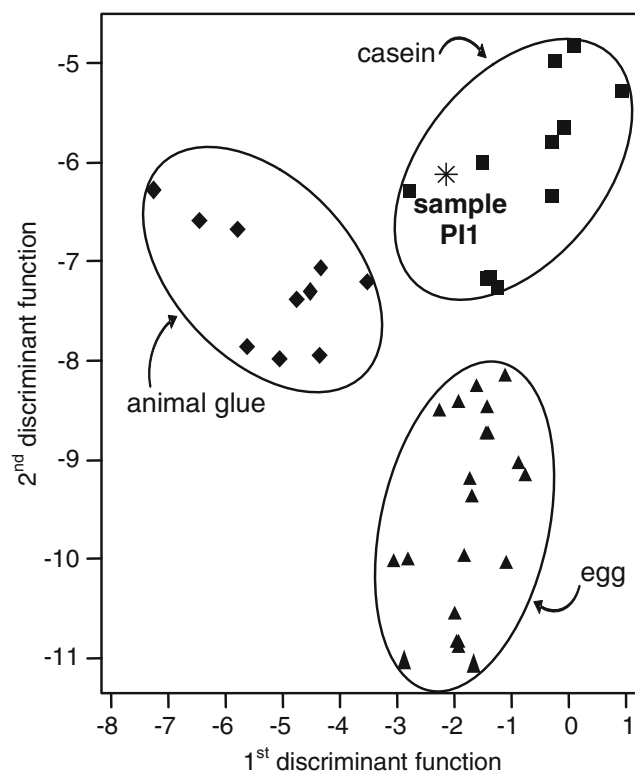


Fig. 14 Plot of the first two discriminant functions for the weight percentages of 14 amino acids (alanine, glycine, valine, leucine, isoleucine, proline, methionine, serine, threonine, phenylalanine, aspartic acid, hydroxyproline, glutamic acid and tyrosine) in the fragment of rock paint PI1, compared with reference painting samples containing proteinaceous binders

Table 6 List of artefacts with traces of colour subjected to chemical analysis

ID	Phase	Type	Residues of colour	Chemical analysis
L1	LA1	Lumps of raw material	Yellow	FTIR, Raman, XRD, visible-NIR, GC-MS
L2	LA2	Lumps of raw material	Yellow	FTIR, Raman, XRD, visible-NIR, GC-MS
L3	LA2	Lumps of raw material	Red	FTIR, Raman, XRD, visible-NIR, GC-MS
L5	LA3	Lumps of raw material	Yellow	FTIR, Raman, XRD, visible-NIR, GC-MS
L6	LA3	Lumps of raw material	Red	FTIR, Raman, XRD, visible-NIR, GC-MS
L7	EP1	Lumps of raw material	Red	FTIR, Raman, XRD, visible-NIR, GC-MS
L8	EP1	Lumps of raw material	Dark yellowish brown	FTIR, Raman, XRD, visible-NIR, GC-MS
L9	EP1	Lumps of raw material	Dark yellowish brown	FTIR, Raman, XRD, visible-NIR, GC-MS
L10	EP1	Lumps of raw material	Red	FTIR, Raman, XRD, visible-NIR, GC-MS
L11	EP1	Lumps of raw material	Yellow	FTIR, Raman, XRD, visible-NIR, GC-MS
L13	EP2	Lumps of raw material	Dusky red	FTIR, Raman, XRD, visible-NIR, GC-MS
L14	EP2	Lumps of raw material	Dark reddish brown	FTIR, Raman, XRD, visible-NIR, GC-MS
L15	EP2	Lumps of raw material	Dark reddish brown	FTIR, Raman, XRD, visible-NIR, GC-MS
L16	EP2	Lumps of raw material	Red	FTIR, Raman, XRD, visible-NIR, GC-MS
L17	MP1	Lumps of raw material	Yellow	FTIR, Raman, XRD, visible-NIR, GC-MS
L18	MP1	Lumps of raw material	Yellow	FTIR, Raman, XRD, visible-NIR, GC-MS
L19	MP2	Lumps of raw material	Dark reddish brown	FTIR, Raman, XRD, visible-NIR, GC-MS
L20	MP2	Lumps of raw material	Dark reddish brown	FTIR, Raman, XRD, visible-NIR, GC-MS
L21	MP2	Lumps of raw material	Dusky red	FTIR, Raman, XRD, visible-NIR, GC-MS
L22	EP1	Lumps of raw material	Dark brown	FTIR, Raman, XRD, visible-NIR, GC-MS
GE1	LA1	Lower grinding stone	Dull yellow	FTIR, Raman, XRD ^a
GE2	LA1	Lower grinding stone	Light bluish grey; yellow; weak red	FTIR, Raman, XRD ^a
GE8	LA2	Lower grinding stone	Light yellow	FTIR, Raman, XRD ^a
GE17	LA2	Lower grinding stone	Red	FTIR, Raman, XRD ^a
GE26	LA2	Lower grinding stone	Purplish grey; pale yellow	FTIR, Raman, XRD ^a
GE27	LA2	Lower grinding stone	Brown	FTIR, Raman, XRD ^a
GE28	LA2	Lower grinding stone	Dark reddish brown	FTIR, Raman, XRD ^a
GE31	LA2	Lower grinding stone	Red	FTIR, Raman, XRD ^a
GE38	LA3	Lower grinding stone	Brownish yellow	FTIR, Raman, XRD ^a
GE39	LA3	Lower grinding stone	Weak red	FTIR, Raman, XRD ^a
GE59	LA3	Lower grinding stone	Pale red; light yellow	FTIR, Raman, XRD ^a
GE60	LA3	Lower grinding stone	Greyish red	FTIR, Raman, XRD ^a
GE61	LA3	Lower grinding stone	Greyish red	FTIR, Raman, XRD ^a
GE63	LA3	Lower grinding stone	Dusky red; bright brown	FTIR, Raman, XRD ^a
GE65	LA3	Lower grinding stone	Pale red; brownish yellow	FTIR, Raman, XRD ^a
GE67	LA3	Lower grinding stone	Bright brown–pale red	FTIR, Raman, XRD ^a
GE68	LA3	Lower grinding stone	Pale red; pale yellow	FTIR, Raman, XRD ^a
GE72	LA3	Lower grinding stone	Pale red; pale yellow	FTIR, Raman, XRD ^a
GE73	LA3	Lower grinding stone	Light red; bright yellowish	FTIR, Raman, XRD ^a
GE74	LA3	Lower grinding stone	Purplish grey; yellow	FTIR, Raman, XRD ^a
GE76	LA3	Lower grinding stone	Reddish brown	FTIR, Raman, XRD ^a
GE80	EP1	Lower grinding stone	Red	FTIR, Raman, XRD ^a
GE94	EP1	Lower grinding stone	Reddish brown; dull yellow	FTIR, Raman, XRD ^a
GE96	EP1	Lower grinding stone	Bright brown–pale red	FTIR, Raman, XRD ^a
GE99	EP1	Lower grinding stone	Light reddish brown	FTIR, Raman, XRD ^a
GE111	MP1	Lower grinding stone	Dark reddish grey	FTIR, Raman, XRD ^a
GE112	MP1	Lower grinding stone	Reddish yellow; bright yellowish	FTIR, Raman, XRD ^a
GE113	MP1	Lower grinding stone	Reddish brown	FTIR, Raman, XRD ^a

Table 6 (continued)

ID	Phase	Type	Residues of colour	Chemical analysis
GE117	MP2	Lower grinding stone	Greyish brown	FTIR, Raman, XRD ^a
GE118	MP2	Lower grinding stone	Light yellowish brown	FTIR, Raman, XRD ^a
GE125	MP2	Lower grinding stone	Pale red	FTIR, Raman, XRD ^a
GE126	MP2	Lower grinding stone	Weak red; yellowish brown; light bluish grey	FTIR, Raman, XRD ^a
GE127	MP2	Lower grinding stone	Purplish grey; yellowish grey	FTIR, Raman, XRD ^a
GE130	MP2	Lower grinding stone	Weak red; pale yellow	FTIR, Raman, XRD ^a
GE131	MP2	Lower grinding stone	Red	FTIR, Raman, XRD ^a
GE132	MP2	Lower grinding stone	Red	FTIR, Raman, XRD ^a
GE135	MP2	Lower grinding stone	Red	FTIR, Raman, XRD ^a
GE137	LP1	Lower grinding stone	Dusky red; light bluish grey; yellow	FTIR, Raman, XRD ^a
GE140	LA2	Lower grinding stone	Red	FTIR, Raman, XRD ^a
GE148	LA3	Lower grinding stone	Reddish brown	FTIR, Raman, XRD ^a
GE152	LA3	Lower grinding stone	Red	FTIR, Raman, XRD ^a
GE153	LA3	Lower grinding stone	Bright brown	FTIR, Raman, XRD ^a
GE155	LA3	UGS	Red	FTIR, Raman, XRD ^a
GE166	EP1	Upper grinding stone	Yellowish red	FTIR, Raman, XRD ^a
GE171	EP1	Upper grinding stone	Yellowish brown	FTIR, Raman, XRD ^a
GE185	EP2	Upper grinding stone	Weak red	FTIR, Raman, XRD ^a
SC12	MP2	Knapped stone with colour	Red	FTIR, Raman, XRD ^a
SC13	MP2	Knapped stone	Yellowish grey	FTIR, Raman, XRD ^a
SC16	LA2	Stone with colour	Red	FTIR, Raman, XRD ^a
SC17	LA3	Stone with colour	Yellow	FTIR, Raman, XRD ^a
SC18	LA3	Stone with colour	Red	FTIR, Raman, XRD ^a
SC20	EP1	Stone with colour	Red	FTIR, Raman, XRD ^a
SC21	EP1	Stone with colour	Yellow	FTIR, Raman, XRD ^a
PI4	MP2	Painted pebble	Reddish brown	FTIR, Raman, XRD ^a
PI5	LP1	Painted pebble	Reddish brown	FTIR, Raman, XRD ^a
PI1	LA2	Fragment of painted rock wall	Reddish brown	GC-MS
OIC3	EP1	Bone with colour	Red	SEM-EDX
OIC9	LA3	Wooden stick	Dark red	Raman

^a GCMS was used to determine the fatty acid distribution for samples GE155 and PI4

with a series of painted films containing different binders prepared in our laboratory (Fig. 14; ESM 2). Also, the distribution of fatty acids in the sample was examined qualitatively, resulting to be significantly different from those observed for the ochre lumps and similar to that described above for the samples from the grinding equipment and from the painted pebble.

Discussion

Origins of the pigments

Hematite and goethite are the most attested mineral pigments used at Takarkori. The latter is largely available in the area,

whereas hematite is less represented. The main sources of Fe-bearing minerals are as follows (Fig. 2): (i) paleosols and pedogenetic Fe-rich crusts, where they are related to clay minerals (Cremaschi and Trombino 1998; Zerboni et al. 2011), (ii) Fe-rich strata of the local rock formations (Galečić 1984; Jakovljević 1984), (iii) banded iron speleothems formed in the tertiary (Zerboni et al. 2014). In one sample (L20), hematite is associated with jarosite ($\text{KFe}^{3+}_3(\text{OH})_6(\text{SO}_4)_2$), which is a mineral never identified in the Tadrart Acacus and poorly known from archaeological contexts in the central Sahara. Some items of the Egyptian Old Kingdom from a British Museum collection are known in literature, and in that case, jarosite was considered as a pure mineral source rather than an alteration product, as instead commonly proposed (Ambers

2004). We interpreted the jarosite from Takarkori as an autochthonous mineral; its formation may be related to post-depositional processes and to the peculiar chemical properties of the anthropogenic deposit of Takarkori. The latter is very rich in organics, which also includes a large amount of sulphur (di Lernia et al. 2012) and potassium (locally precipitated as nitre), the latter originating from the diagenesis of wood ash (Biagetti and di Lernia 2013; di Lernia and Tafuri 2013; Cremaschi et al. 2014). Jarosite may have precipitated after the weathering at low temperature of Fe hydroxides in the acidic environment of the anthropogenic deposit (Bladh 1982; Keene et al. 2010).

Colour in context: pigments, tools and spaces

The analyses demonstrated that the pigments were treated following specific processes, some of them archaeologically and chemically identified: e.g. the addition of fatty substances, intentional heating and dilution with liquids (water?). The supporting elements were stones of different shapes and sizes, all made from local quartzarenite. The grinding equipment clearly reveals an opportunistic use and continuous activity of recycling until discard. The colour on the stones, principally red, could potentially have covered the entire surface, and in a few cases, both faces show residues of colour. Stone tools, generally scrapers, were used to scratch the pigments and grinding stones to crush them. The distribution of coloured residues on the grinding equipment clearly shows that lower and upper grinding stones have a similar trend according to the cultural phases (Table 1; ESM 1); furthermore, it appears that the former may have residues of different colours (up to three), whereas the upper grinding stone normally shows only one colour. These elements may suggest a multiple function for the lower passive stones: not only as bases for crushing and pulverization of the pigments but possibly also as “palette” for the application of the paint itself (see Fig. 3d).

Chemical investigation of a fragment of the vault with a faded painted subject of late pastoral age indicated that the prehistoric artisans added casein to the pigments. In our case, the combination of a rapid burial of the painted slab with the vicinity of the vault may have prevented further contamination processes and then favoured its preservation. Milking is well attested in the region, as shown by residue analysis on Takarkori potsherds, at least from the Middle Pastoral (Dunne et al. 2012). This is not the first time that Acacus artworks yielded evidence for the use of binders, either casein or albumin (Mori 1965; Mori et al. 2006). This is indeed a debated issue, especially when compared to the evidence from the neighbouring massif of the Tassili, where no traces of binders have yet been found (Hachid et al. 2012). Also, in the Wadi Sura area, the western Gilf Kebir in Egypt, it is not clear if binders were added to ochre or alternatively, if their preservation was heavily compromised (Krause et al. 2013).

Given the small size and weight of samples from grinding stones, it has not been possible to test if some of them contained traces of organic binder. Together with the state of preservation and local taphonomic processes, this is still a serious obstacle to fully understand this issue.

Notwithstanding the continuous reuses and reoccupations of the same area through time, which make primary and functional positions very difficult to detect, thanks to the extensive excavations and the meticulous sieving of all the sediment, it was possible to identify at least 4 “workshops” for ochre processing, a rather rare evidence for this type of living site. They date to different cultural phases (LA, EP and MP) and boost our understanding of the ancient lifestyles of Takarkori inhabitants.

Using colour: decorating objects, painting walls

Out of 256 artefacts with traces of colour, only 11 at Takarkori are coloured (“passive”) objects: the three painted fragments of wall (PI1, PI2, PI3), a couple of pebbles (PI4, PI5), three bone tools (OIC1, OIC2, OIC6), one wooden stick (OIC9), one plaque in shale (SC23) and a ceramic ring (OIC 10). This is to say that the archaeological record at Takarkori provides a strong evidence and in-depth information about colour processing (“active” elements) but scarce data on its final use (“passive” elements).

In a sense, the *chaîne opératoire* (if only one) seems to be partially visible archaeologically, also because the walls of the shelter have been extensively eroded by wind and any rock paintings would have been completely lost.

Nevertheless, we have chemical evidence to show that some of the lumps of minerals were processed using fats or oils, while a proteinaceous binder was found in the fragment of rock painting. We record a difference in the chemical distribution between lumps of minerals and pigment from rock paintings. If this is effectively related to different functions of the colours and not to weathering or degradation, then the “sticky” lumps with addition of fatty materials at Takarkori are not connected to the parietal art, neither to the painting of portable objects. Among the possible known uses of crushed minerals—both ethnographically and archaeologically—we recall here the consumption of ochre mixed with other elements such as medicine (Mahaney et al. 1993), the use as mastic for hafting lithic tools and to repair wooden items, the preparation (normally mixed with butter or milk) to protect and/or decorate hair and skin (Rudner 1982; Wadley 2001), funerary treatment (e.g. Roche 1963) and many others (see a recent review by Rifkin 2011, 2012). At least at Takarkori, very few lithic tools show traces of mastic (but no ochre found), and no evidence is known from other Acacus and Messak sites. The several inhumations buried in a recessed part of the shelter, dated from ca. 8000 to 4500 uncal bp, show no traces of ochre. The use of ochre in funerary contexts is a

cultural habitus well known from Pleistocene and Early Holocene contexts in Northern Africa (e.g. Belcastro et al. 2010; Mariotti et al. 2014) but completely absent in the Acacus and Messak record (e.g. di Lernia and Manzi 1998; di Lernia et al. 2012) and more generally in the larger Sahara. Therefore, considering the lack of archaeological evidence for the use of these sticky lumps, we should consider other functions whose outcomes are perishable and/or invisible in the archaeological record (e.g. medicine, hair and body decoration, etc.). In this perspective, body decoration and body tattoos are serious candidates but difficult to prove. The only circumstantial evidence may come from pictorial details in many Round Head and Pastoral paintings, where body decoration is common (e.g. Mori 1965; Sansoni 1994; Soleihavoup 2007).

If the lumps of minerals with a sticky consistence and small size were used for particular purposes which have yet to be defined, what was the function of the large quantity of pulverized pigments found on the hundreds of grinding stones? In our perspective, despite the absence of parietal art on the Takarkori vault, abraded by millennia of severe erosion, the most parsimonious explanation for such a massive presence of coloured residues is indeed the making of parietal paintings.

Final remarks

The presence of coloured residues on artefacts from Holocene sites in the Tadrart Acacus Mountains and surroundings is not uncommon but mostly related to “active” items, i.e. artefacts used to crush, grind, mix or spread the pigments. Yet, the rich assemblage from Takarkori gives us the opportunity to reconstruct the use of pigments over a long chronological interval, from ca. 8900 to 4500 uncal bp, which encompasses different foragers’ and herders’ cultural traditions. Given the outstanding importance of Acacus rock art sites, there was in the past a certain tendency to equate the presence of colour on artefacts to parietal art (di Lernia 2012). Here, we have analysed different segments of the archaeological record, showing the mechanisms of procurement and processing of pigments, and their potential use. Ochre was shown to have been reasonably used for personal use (especially the lumps mixed with fat or plant oils), to decorate stones, slabs, bone, wooden and ceramic artefacts, and very likely to prepare the basis for the paint. However, for this last point, there is no definitive evidence of the relation between the coloured residues on grinding stones and parietal rock art. Furthermore, we have no evidence of rock art on the shelter wall, but for the items fallen and buried in the deposit, therefore, no taphonomic process could be tested.

The rarity of coloured “passive” items, i.e. painted artefacts, the absence of stone tools showing the use of ochre as adhesive and the lack of ochre on skeletal remains at the site

sharply contrast against the simultaneous abundance of artefacts, especially grinding stones, with coloured residues. This leads us to suggest a primary, but not exclusive, use of ochre and other pigments found on the grinding stones as raw materials for parietal rock art. This is true for Takarkori, but it might stand, we believe, for the entire Acacus area.

If this circumstantial reasoning were plausible, then we should emphasize the wealth of artefacts with coloured residues already in the Late Acacus contexts, from around 8900 uncal bp. Approximately 100 grinding stones were used during these phase to process the pigments and prepare the colours. Even though the evidence is indirect, it seems likely to relate this presence also to the making of parietal artworks. The wooden spatula from Uan Afuda from an 8500-year-old layer, with sticky reddish pigment on its edge and the grinding stones with coloured residues from other Late Acacus contexts, such as Uan Tabu, Fozziagiaren and Ti-n-Torha, may be considered as pieces of an ongoing puzzle (di Lernia 1999; di Lernia 2012; Gallinaro *in press*).

To conclude, despite the harsh, often acrimonious debate which unfortunately characterized the research on rock art and related aspects in the Sahara (Smith 2013), there is yet good opportunities to understand how Holocene Saharans used ochre and other minerals, not only for rock paintings but also body care, tattoos and decoration of personal ornaments.

Acknowledgments The research is part of the activities of the Italian-Libyan Archaeological Mission in the Acacus and Messak (central Sahara), Sapienza University of Rome and Department of Archaeology, Tripoli, directed by Savino di Lernia. Funds are provided by Grandi Scavi di Ateneo, Sapienza University of Rome and Italian Minister of Foreign Affairs—DGPS, entrusted to SDL.

SDL designed the research, directed the fieldwork, including sampling, studied the archaeological assemblage and wrote the paper. SB performed chemical analyses and wrote the relevant parts of the paper. IC and VG contributed to the chemical experiments. MC and AZ provided information on the geological context. MG contributed to the background of rock art evidence, analysed the painted artwork and contributed to the archaeological analysis. GP studied the grinding equipment in the field. AMM studied the archaeobotanical context. Discussion and conclusion are due to all authors. We thank all Libyan authorities for their help and support. We warmly thank the following colleagues: Stefano Biagetti and Emanuele Cancellieri for their support; Francesca Tuccillo, Diego Belotti and Andrea Mazzochin for their contribution to chemical analyses; and Italo Campostrini for SEM-EDX observation. Our warmest thanks to Sara Giovannetti for the photographic documentation. We wish to warmly thank the two anonymous reviewers who commented on a previous draft of the manuscript and greatly improved the present version of the paper.

Conflict of interest The authors declare no conflict of interests.

References

- Ambers J (2004) Raman analysis of pigments from the Egyptian Old Kingdom. *J Raman Spectrosc* 35:768–773

- Barich BE (ed) (1987) Archaeology and environment in the Libyan Sahara. The excavations in the Tadrart Acacus, 1978-1983 vol 368. BAR, Oxford
- Barich BE, Mori F (1970) Missione paleontologica italiana nel Sahara libico. Risultati della campagna 1969. *Origini* IV:79–142
- Barth H (1857–1858) *Reisen und Entdeckungen in Nord und Central Africa in den Jahren 1849 bis 1855* (5 vols.). Justus Perthes, Gotha
- Belcastro MG, Condemi S, Mariotti V (2010) Funerary practices of the Iberomaurosian population of Taforalt (Tafoughalt, Morocco, 11–12,000 BP): the case of Grave XII. *J Hum Evol* 58:522–532. doi:10.1016/j.jhevol.2010.03.011
- Biagetti S, di Lernia S (2013) Holocene fillings of Saharan rock shelters: the case of Takarkori and other sites from the Tadrart Acacus Mts. (SW Libya). *Afr Archaeol Rev* 30:305–328
- Bikiaris D, Daniilia S, Sotiropoulou S, Katsimbiri O, Pavlidou E, Moutsatsou AP, Chrysosoulakis Y (1999) Ochre differentiation through micro-Raman and micro-FTIR spectroscopies: application on wall paintings at Meteora and Mount Athos, Greece. *Spectrochim Acta* 56:3–18
- Bladh K (1982) The Formation of Goethite, Jarosite, and Alunite during the Weathering of Sulfide-Bearing Felsic Rocks. *Econ Geol* 77:176–184
- Cherkinsky A, di Lernia S (2013) Bayesian approach to 14C dates for estimation of long-term archaeological sequences in arid environments: the Holocene Site of Takarkori Rockshelter, Southwest Libya. *Radiocarbon* 55:771–782
- Copley MS, Rose PJ, Clapham A, Edwards DN, Horton MC, Evershed RP (2001) Detection of palm fruit lipids in archaeological pottery from QasrIbrim, Egyptian Nubia. *Proc R Soc Lond B* 268:593–597
- Copley MS, Bland HA, Rose P, Horton M, Evershed RP (2005) Gas chromatographic, mass spectrometric and stable carbon isotopic investigations of organic residues of plant oils and animal fats employed as illuminants in archaeological lamps from Egypt. *Analyst* 130:860–871
- Cremaschi M, di Lernia S (eds) (1998) *Wadi Teshuinat. Palaeoenvironment and prehistory in South-western Fezzan (Libyan Sahara)*. Quaderni di Geodinamica Alpina e Quaternaria, vol 7. CNR, Milano
- Cremaschi M, Trombino L (1998) The palaeoclimatic significance of the paleosols in southern Fezzan (Libyan Sahara): morphological and micromorphological aspects. *Catena* 34:131–156
- Cremaschi M, Zerboni A, Mercuri AM, Olmi L, Biagetti S, di Lernia S (2014) Takarkori rock shelter (SW Libya): an archive of Holocene climate and environmental changes in the central Sahara. *Quat Sci Rev* 101:36–60. doi:10.1016/j.quascirev.2014.07.004
- D'Elboux Bernardino N, SevilhanoPuglieri T, de Faria DLA (2014) Effect of MnO₂ and α-Fe₂O₃ on organic binders degradation investigated by Raman spectroscopy. *Vib Spectrosc* 70:70–77
- de Faria DLA, Lopes FN (2007) Heated goethite and natural hematite: can Raman spectroscopy be used to differentiate them? *Vib Spectrosc* 45:117–121
- de Faria DLA, Venancio Silva S, de Oliveira MT (1997) Raman microspectroscopy of some iron oxides and oxyhydroxides. *J Raman Spectrosc* 28:873–878
- di Lernia S (ed) (1999) *The Uan Afuda Cave: Hunter-Gatherers Societies of Central Sahara*. AZA Monographs, vol 1. All'Insegna del Giglio, Firenze
- di Lernia S (2005) Incoming tourism, outgoing culture: tourism, development and cultural heritage in the Libyan Sahara. *J N Afr Stud* 10:441–457
- di Lernia S (2012) Thoughts on the rock art of the Tadrart Acacus Mts., SW Libya. *Adoranten* 19–37
- di Lernia S, Gallinaro M (2010) The date and context of Neolithic rock art in the Sahara: engravings and ceremonial monuments from Messak Settafet (south-west Libya). *Antiquity* 84:954–975
- di Lernia S, Gallinaro M (2011) Working in a UNESCO WH site. Problems and practices on the rock art of the Tadrart Acacus (SW Libya, central Sahara). *J Afr Archaeol* 9:159–175
- di Lernia S, Manzi G (1998) Funerary practices and anthropological features at 8000-5000 BP. Some evidence from central-southern Acacus (Libyan Sahara). In: Cremaschi M, di Lernia S (eds) *Wadi Teshuinat: Palaeoenvironment and Prehistory in South-western Fezzan (Libyan Sahara)*. C.N.R., Milano, pp 217–242
- di Lernia S, Tafuri MA (2013) Persistent deathplaces and mobile landmarks. The Holocene mortuary and isotopic record from Wadi Takarkori (SW Libya). *J Anthropol Archaeol* 32:1–15
- di Lernia S, Zampetti D (eds) (2008) *La Memoriadell'arte. La Memoria dell'Arte. Le Pitture Rupestri dell'Acacus tra Passato e Futuro. All'Insegna del Giglio*, Firenze
- di Lernia S, Massamba N'siala I, Mercuri AM (2012) Saharan prehistoric basketry. Archaeological and archaeobotanical analysis of the early-middle Holocene assemblage from Takarkori (Acacus Mts., SW Libya). *J Archaeol Sci* 39:1837–1853
- di Lernia S et al (2013) Inside the “African Cattle Complex”: animal burials in the Holocene Central Sahara. *PLoS One* 8:e56879. doi:10.1371/journal.pone.0056879
- Dunne J et al (2012) First dairying in ‘Green’ Saharan Africa in the 5th Millennium BC. *Nature* 486:390–394
- Gadsden JA (1975) *Infrared spectra of minerals and related inorganic compounds*. Butterworths, London
- Galečić M (1984) Geological map of Libya, explanatory booklet, sheet: Anay, NG 32-16, scale 1:250000. Industrial Research Centre, Tripoli
- Gallinaro M (2013) Saharan rock art: local dynamics and wider perspectives. *Arts* 2:350–382
- Gallinaro M (in press) Rock art landscape of the central Saharan massifs: a contextual analysis of Round Heads style. In: Gutierrez et al. (ed) *Proceedings of the International Colloquium, Rock art of Africa Paris, 15, 16 and 17 January 2014*
- Garcea EAA (ed) (2001) *Uan Tabu: in the settlement history of the Libyan Sahara*. AZA Monographs 2. All'Insegna del Giglio, Firenze
- Garcea EAA, Sebastiani R (1998) Middle and Late Pastoral Neolithic from the Uan Telocatrockshelter, Tadrart Acacus (Libyan Sahara). In: Cremaschi M, di Lernia S (eds) *Wadi Teshuinat—palaeoenvironment and prehistory in south-western Fezzan (Libyan Sahara)*. CNR, Roma-Milano, pp 201–216
- Gialanella S, Belli R, Dalmeri G, Lonardelli I, Mattarelli M, Montagna M, Toniutti L (2011) Artificial or natural origin of hematite-based red pigments in archaeological contexts: the case of Riparo Dalmeri (Trento, Italy). *Archaeometry* 53:950–962
- Guagnin M (2012) From savanna to desert: rock art and the environment in the Wadi al-Hayat (Libya). In: Huyge D, van Noten F, Swinne D (eds) *The signs of which times? Chronological and palaeoenvironmental issues in the rock art of Northern Africa*. Royal Academy for Overseas Sciences, Brussels, pp 145–157
- Hachid M et al (2012) Quelques résultats du projet de datation directe et indirecte de l'art rupestre Saharien. In: Huyge D, Van Noten F, Swinne D (eds) *The signs of which times? Chronological and palaeoenvironmental issues in the rock art of Northern Africa*. Royal Academy for Overseas Sciences, Bruxelles, pp 71–96
- Harmann J (2005–2013) DStretch. Web Site for the DStretch plugin to ImageJ. DStretch. A tool for the digital enhancement of pictographs. <http://www.dstretch.com/>. Accessed June 2014
- Jakovlječić Ž (1984) Geological map of Libya. Explanatory booklet, sheet: Al Awaynat, NG 32-12, scale 1:250000. Socialist People's Libyan Arab Jamahiriya, Tripoli
- Keene A, Johnston S, Bush R, Sullivan L, Burton E (2010) Reductive dissolution of natural jarosite in a tidally inundated acid sulfate soil: geochemical implications. In: *19th World Congress of Soil Science, Soil Solutions for a Changing World, 1-6 August 2010, Brisbane, Australia.*, pp 100–103

- Krause S, Riemer H, Leisen S (2013) Paints and pigments in the rock art of Wadi Sura. In: Kuper R (ed) Wadi Sura—the cave of beasts. A rock art site in the Gilf Kebir (sw Egypt), vol Africa Praehistorica 26. Heinrich Barth Institute, Köln, pp 58–61
- Kuper R (ed) (2013) Wadi Sura: the cave of beasts; a rock art site in the Gilf Kebir (SW-Egypt). Africa Praehistorica, vol 26. Heinrich-Barth-Institut, Köln
- Kustova GN, Burgina EB, Sadikov VA, Poryvaev SG (1992) Vibrational spectroscopic investigation of the goethite thermal decomposition products. *Phys Chem Miner* 18:379–382
- Le Quellec JL (1998) Art Rupestre et Préhistoire du Sahara. Le Messak Libyen. Bibliothèque Scientifique Payot, Paris
- Le Quellec JL (2013) A new chronology for Saharan rock art. In: Malla B (ed) The world of rock art: an overview of the five continents. Aryan Books International, New Delhi, pp 23–44
- Mahaney W, Hancock RGV, Inoue M (1993) Geochemistry and clay mineralogy of soils eaten by Japanese macaques. *Primates* 34:85–91
- Maier MS, de Faria DLA, Boschini MT, Parera SD, del Castillo Bernal MF (2007) Combined use of vibrational spectroscopy and GC-MS methods in the characterization of archeological pastes from Patagonia. *Vib Spectrosc* 44:182–186
- Mariotti V, Condemni S, Belcastro MG (2014) Iberomaurusian funerary customs: new evidence from unpublished records of the 1950s excavations of the Tafoult necropolis (Morocco). *J Archaeol Sci* 49:488–499. doi:10.1016/j.jas.2014.05.037
- Mercuri AM (2008) Human influence, plant landscape evolution and climate inferences from the archaeobotanical records of the Wadi Teshuinat area (Libyan Sahara). *J Arid Environ* 72:1950–1967
- Mills JS, White R (1994) The organic chemistry of museum objects. Butterworths, London
- Mittet GR (1980) The degradation of tall oil fatty acids by molecular oxygen in alkaline media. *Diss Abstr Int B* 41:1373
- Moioli P, Seccaroni C (1992) Esame delle tracce di pigmenti su alcuni frammenti di dipinti rupestri. In: Lupaccioli M (ed) Arte e Culture del Sahara preistorico. Qasar, Università degli Studi di Roma «La Sapienza», Roma, pp 109–110
- Mori F (1965) Tadrart Acacus. *Arte Rupestre e Culture del Sahara Preistorico*. Einaudi, Torino
- Mori F, Ponti R, Messina A, Flieger M, Havlicek V, Sinibaldi M (2006) Chemical characterization and AMS radiocarbon dating of the binder of a prehistoric rock pictograph at Tadrart Acacus, southern west Libya. *J Cult Herit* 7:344–349
- Morris RV, Lauer HV, Lawson CA, Gibson EK, Nace GA, Stewart C (1985) Spectral and other physicochemical properties of submicron powders of hematite (α -Fe₂O₃), maghemite (γ -Fe₂O₃), magnetite (Fe₃O₄), goethite (α -FeOOH) and lepidocrocite (γ -FeOOH). *J Geophys Res* 90:3126–3144
- Mortimore JL, Marshall LR, Almond MJ, Hollins P, Matthews W (2004) Analysis of red and yellow ochre samples from Clearwell caves and Catalhöyük by vibrational spectroscopy and other techniques. *Spectrochim Acta A* 60:1179–1188
- Muzzolini A (2001) Saharan Africa. In: Whitley DS (ed) Handbook of rock art research. AltaMira Press, Walnut Creek, pp 605–636
- Onoratini G, Perinet G (1985) Données minéralogiques sur les colorants rouges préhistoriques de Provence: démonstration que certains d'entre eux ont été obtenus par calcination de goethite. *C R Acad Scie Sér 2* 301:119–124
- Pomiès MP, Morin G, Vignaud C (1998) XRD study of goethite-hematite transformation: application to the identification of heated prehistoric pigments. *Eur J Solid State Inorg Chem* 35:9–25
- Ponti R (1995) Painted grinding stone from the Uan Amil shelter (Tadrart Acacus—Libya). *Quat Nova V*:171–186
- Rampazzi L, Cariati F, Tanda G, Colombini MP (2002) Characterisation of wall paintings in the SosFurighesos necropolis (Anela, Italy). *J Cult Herit* 3:237–240
- Rampazzi L, Campo L, Cariati F, Tanda G, Colombini MP (2007) Prehistoric wall paintings: the case of the Domus de Janas necropolis (Sardinia, Italy). *Archaeometry* 49:559–569
- Regert M, Bland HA, Dudd SN, van Bergen PF, Evershed RP (1998) Free and bound fatty acid oxidation products in archaeological ceramic vessels. *Proc R Soc Lond B* 265:2027–2032
- Rifkin R (2011) Assessing the efficacy of red ochre as a prehistoric hide tanning ingredient. *J Afr Archaeol* 9:131–158
- Rifkin R (2012) The symbolic and functional exploitation of ochre during the South African Middle Stone Age, PhD Dissertation, University of Johannesburg, <http://wiredspace.wits.ac.za/handle/10539/11832>
- Roche J (1963) L'Épipaléolithique marocain. Paris
- Rudner I (1982) Khoisan pigments and paints and their relationships to rock paintings. *Annals of the South African Museum* 87. South African Museum, Cape Town
- Sansoni U (1994) Le più antiche pitture del Sahara. L'arte delle Teste Rotonde. Jaka Book, Milano
- Shimoyama A, Hayakawa K, Harada K (1993) Conversion of oleic acid to monocarboxylic acids and γ -lactones by laboratory heating experiments in relation to organic diagenesis. *Geochem J* 27:59–70
- Shimoyama A, Kisu N, Harada K, Wakita S, Tsuneki A, Iwasaki T (1995) Fatty acid analysis of archeological pottery vessels excavated in Tell Mastuma, Syria. *Bull Chem Soc Jpn* 68:1565–1568
- Smith B (2013) Rock art research in Africa. In: Lane P, Mitchell P (eds) Handbook of African archaeology. Oxford University Press, Oxford, pp 145–162
- Soleihavouf F (2007) L'art mystérieux des Têtes Rondes au Sahara. Fatou, Paris
- Tafuri MA, Bentley RA, Manzi G, di Lernia S (2006) Mobility and kinship in the prehistoric Sahara: strontium isotope analysis of Holocene human skeletons from the Acacus Mts. (southwestern Libya). *J Anthropol Archaeol* 25:390–402
- Udda M, Sassa S, Yoshimura S, Kondo J, Nakamura M, Ban Y, Adachi H (2000) Yellow, red and blue pigments from ancient Egyptian palace painted walls. *Nucl Inst Methods Phys Res B* 161–163:758–761
- van der Marel HW, Beutelspacher H (1976) Atlas of infrared spectroscopy of clay minerals and their admixtures. Elsevier, Amsterdam
- Wadley L (2001) What is cultural modernity? A general view and a south African perspective from Rose cottage cave. *Camb Archaeol J* 11:201–221
- Zerboni A (2012) Rock art from the central Sahara (Libya): a geoarchaeological and palaeoenvironmental perspective. In: Huyge D, Van Noten F, Swinne D (eds) The signs of which times? Chronological and palaeoenvironmental issues in the rock art of Northern Africa. Royal Academy for Overseas Sciences, Bruxelles, pp 175–195
- Zerboni A, Trombino L, Cremaschi M (2011) Micromorphological approach to polycyclic pedogenesis on the Messak Settafet plateau (central Sahara): formative processes and palaeoenvironmental significance. *Geomorphology* 125:319–335
- Zerboni A, Perego A, Cremaschi M (2014) Geomorphological map of the Tadrart Acacus massif and the Erg Uan Kasa (Libyan Central Sahara). *J Maps*. doi:10.1080/17445647.2014.955891